

## Supplemental Material

### Supplemental Results and Discussion

#### No regulatory role for REST in human heart failure

REST (RE1 silencing transcription factor) is a nuclear protein that binds to a conserved 23 bp motif known as RE1 (repressor element 1, also called NRSE) in a large number of genes encoding neuronal traits such as ion channels, synaptic vesicle proteins, and neurotransmitter receptors (1, 2). In animal models, REST was also identified as a key regulator of fetal genes in the adult heart, including ANP and BNP (3-6). REST silences genes by recruiting histone modifying proteins (e.g., HDACs, G9a, SUV39H1 and LSD1) to its target genes (6). In mice exposed to pressure overload, the increase of BNP correlated with downregulation of REST gene expression (4). Moreover, transgenic expression of a dominant-negative mutant of REST in mouse hearts induced dilated cardiomyopathy (4). The role of REST in human heart failure, however, has never been assessed. Therefore, we analyzed expression and localization of REST in human myocardium. In contrast to results from mice with pressure-induced hypertrophy (4), mRNA levels of REST were unchanged in human failing myocardium (Figure S4A). Furthermore, protein expression of REST, which was detected only in the nuclear, but not the cytosolic fraction, was unchanged in failing versus nonfailing myocardium (Figure S4B). Finally, REST associated with the promoter regions of its target genes ANP and BNP, but not GAPDH. This association, however, was not differentially regulated in failing versus nonfailing myocardium (Figure S4C). The reasons for the differences between our human data and those of experimental systems (3-5, 7) are presently unresolved. As one possible explanation, it has been observed that endogenous REST target genes (as examined in our study) and transiently transfected templates, as commonly used in *in vitro* studies (3-5, 7), recruit different REST-associated multi-protein complexes, with differential impacts on epigenetic modifications (8).

#### Similar effects of cardiac pre- and afterload on ANP expression

In a recent study, differential effects of cardiac pre- and afterload on LV remodelling *in vivo* and fetal gene expression were reported (9). Furthermore, CaMKII was activated only after an increase of afterload, but not preload (9). These data are in seeming contrast to our results that in response to an increase of either pre- or afterload, nuclear HDAC4 export and ANP gene activation were of similar degrees (Figure 8) and induced similar epigenetic patterns (Figures 9 and S6). However, changes in ANP were not reported in the study by Toischer et al. (9), and in our experiments, BNP did not increase after 90 min of elevated pre- or afterload, in agreement with the observation that ANP increases earlier than BNP after aortic banding in mice (10). Differential responses to cardiac pre- and afterload in the two studies may be related to differences in the experimental systems. In our experiments, cardiac pre- and afterload could be controlled independently in the working heart apparatus, and afterload was kept constant when preload was increased (Figure 8C). In contrast, by creating a shunt between the aorta and vena cava inferior in the study by Toischer et al. (9), cardiac afterload may decrease while preload is increased, as we discussed previously (11). Finally, in our experiments, cardiac preload *in vitro* was increased to 30 mmHg, a value that is frequently obtained during cardiac decompensation in patients with heart failure, while in the study by Toischer et al. (9), preload was increased to ~12 mmHg. Finally, systemic effects (i.e. neuroendocrine activation) are avoided in our working heart set-up, but present *in vivo*. Taken together, a more severe increase of preload together with maintained afterload, and possibly the elimination of systemic (neuroendocrine) effects, may account for more prominent effects of preload elevation in our study compared to the study by Toischer et al. (9).

## Detailed Methods

### **Western blot analysis**

Left ventricular (LV) tissue was minced in liquid nitrogen and resuspended in 600 µl cytosolic lysis buffer (in mmol/L: Hepes 10 [pH 7.9], KCl 10, EDTA 0.1, EGTA 0.1, DTT 1, PMSF 0.5). After 15 min of swelling, 25 µl of 10% NP40 was added. The nuclear pellet was resuspended in 200 µl nuclear lysis buffer (in mmol/L: Hepes 20 [pH 7.9], NaCl 0.4, EDTA 1, EGTA 1, DTT 1, PMSF 1). 50 µg (for mouse) or 100 µg of protein (for human) from cytosolic and nuclear extracts was separated on 8% SDS-PAGE and electrophoretically transferred to nitrocellulose membranes (0.2 µm pore size, Schleicher and Schuell, Dassel, Germany). Membranes were blocked in Tris-buffered saline (TBS) containing 5% nonfat dry milk for 120 min at room temperature and exposed to rabbit polyclonal IgG HDAC4 (H-92: sc-11418, Santa Cruz Biotechnology, CA, USA; dilution: 1:1000) mouse monoclonal IgG GAPDH (6C5: sc-32233, Santa Cruz Biotechnology, CA, USA; 1:2000), mouse monoclonal Anti-RNA polymerase II IgG (CTD4GH8: 05-623, Millipore; 1:2000) or rabbit polyclonal IgG REST (NRSF H-290: sc-25398, Santa Cruz Biotechnology; 1:1000). Secondary antibodies (goat anti-rabbit (Sigma-Aldrich, Deisenhofen, Germany; 1:2500 or goat anti-mouse, 170-6516 Bio-Rad, Germany; 1:2500) were incubated for 60 min at room temperature. Proteins were visualized by enhanced chemiluminescence according to the manufacturer's guidelines (Amersham Pharmacia Biotech, Freiburg, Germany), quantified by imaging densitometry and analyzed by the „ImageQuant-TM“ Software (Image Quant, Molecular Dynamics, Krefeld, Germany). Data are presented as intensity optical density (IOD). In all experiments, NF, ICM and DCM tissues were compared by western blot analysis at the same time with identical conditions and separated on the same SDS-PAGE. Different background color of autoradiographs is related to different exposure times, depending on endogenous protein concentrations.

The membranes were stripped two times for 15 minutes at 56°C using stripping buffer (62.5 mM Tris-HCl (pH 6.8), 2% SDS, 0.1 M β-mercaptoethanol), then thoroughly washed with 1xPBS (in mmol/L: NaCl 170, KCl 33, Na<sub>2</sub>HPO<sub>4</sub> 40 and KH<sub>2</sub>PO<sub>4</sub> 18, pH 7.2) for one hour and blocked again in Tris-buffered saline (TBS) containing 5% nonfat dry milk for 120 min at room temperature.

### **RNA Isolation and Reverse Transcription**

RNA was prepared from either human or mouse LV myocardium or rat cardiac myocytes using peqGold TriFast (PeqLab, Erlangen, Germany) extraction reagent according to the manufacturer's protocol. RNA from neonatal rat cardiomyocytes was prepared by using High Pure RNA Isolation Kit (Roche, Germany). For cDNA preparation, 2 µg of RNA was digested with Deoxyribonuclease I (PeqLab). Reverse transcription was conducted using the HighCap cDNA RT Kit (Applied Biosystems, Darmstadt, Germany) according to the manufacturer's protocol.

### **Quantitative Real-Time PCR and Taq-Man PCR**

Quantitative real-time PCR was conducted for gene expression experiments in an ABI PRISM 7700 (Applied Biosystems, Germany) using SYBR Green PCR Mastermix (Applied Biosystems). Threshold cycle (Ct) values were determined using the Sequence Detector 1.7 software. The forward and reverse primers are shown in Table S2 of the Online Supplement. Alternatively, TaqMan PCR was conducted in a StepOne plus thermocycler (Applied Biosystems, Germany) using TaqMan Gene Expression Mastermix (Applied Biosystems). TaqMan Gene Expression Assay numbers (purchased from Applied Biosystems) are shown in Table S3 of the Online Supplement. Threshold cycles (Ct)-Values were calculated with the comparative Ct-method (12). Sequence information of ChIP primers flanking the promoter region are listed in Table S6 and Figure S1.

### **Chromatin Immunoprecipitation (ChIP) assays**

LV myocardium was pulverized in liquid nitrogen, resolved in 1 ml phosphate buffered saline (PBS, in mmol/L: NaCl 170, KCl 33, Na<sub>2</sub>HPO<sub>4</sub> 40 and KH<sub>2</sub>PO<sub>4</sub> 18, pH 7.2) and cross-linked by addition of formaldehyde (1% final concentration) for 10 min. Cross-linking was terminated by adding glycine (125 mmol/L final concentration). The pellets were washed twice with cold PBS and centrifuged for 5 minutes. The Pellets were then resuspended in lysis buffer consisting of 5 mmol/L PIPES, pH 8.0, 85 mmol/L KCL, and 0.5% Igepal CA-630, containing complete protease inhibitors cocktail (Roche, Mannheim, Germany; no. 04693159001) and incubated for 10 min on ice. Nuclei were collected by centrifugation and resuspended in nuclear lysis buffer (50 mmol/L Tris [pH 8.1], 10 mmol/L EDTA, 1% SDS) containing complete protease inhibitors and incubated for 10 min on ice. The chromatin was sonicated (Branson Sonifier 250; Duty Cycle 30 bursts/min, Output Control 3), chilled on ice and centrifuged. The supernatant was transferred into a new reaction tube and diluted five-fold with cold ChIP-buffer (0.01% SDS, 1.1% Triton X-100, 1.2 mmol/L EDTA, 16.7 mmol/L Tris [pH 8.1], 167 mmol/L NaCl) containing complete protease inhibitors. The sheared chromatin was incubated with 40 µl of protein A sepharose (Amersham Biosciences) for 2 hours at 4°C with agitation to reduce non-specific background, centrifuged, and the supernatant fraction was collected. Twenty per cent of the total supernatant was saved to use as a total input control. The chromatin solutions were divided into aliquots and incubated overnight at 4°C with 4 µg of antibody. Antibodies used for immunoprecipitation were:

- anti-acetylK27 (ab4729)
- anti-acetyl H3K9 (ab10812)
- anti-acetyl H4K91 (ab4627)
- anti-dimethyl H3K9 (ab7312)
- anti-trimethyl H3K9 (ab8898)
- anti-trimethyl H3K27 (ab6002)
- anti-dimethyl H3K4 (ab32356)
- anti-trimethyl H3K4 (ab8580)
- anti-JMJD1A (ab52002)
- anti-JMJD2A (ab24545 for human)
- anti-JMJD2A (ab70786 for mouse; all Abcam, Cambridge, UK, respectively)
- anti HP1 $\alpha$  (Millipore, #05-689), and
- anti-REST (upstate, #07-579).

As control for unspecific antibody binding either no antibody was added (for human ChIP-assays) or non-specific IgG (for mouse and rat ChIP-assays; Santa Cruz, sc-2025) was added. The immunocomplexes were collected via incubation with 30 µl of protein A sepharose for at least 3 hours at 4°C with agitation. The beads were consequently washed three times with low salt wash buffer (0.1% SDS, 1% Triton X-100, 2 mmol/L EDTA, 20 mmol/L Tris [pH 8.1], 150 mmol/L NaCl) at 4°C, once with high salt wash buffer (0.1% SDS, 1% Triton X-100, 2 mmol/L EDTA, 20 mmol/L Tris [pH 8.1], 500 mmol/L NaCl) at 4°C, and once with LiCl wash buffer (0.25 mol/L LiCl, 1% Igepal, 1% deoxycholate, 1 mmol/L EDTA, 10 mmol/L Tris [pH 8.0]) and twice with Tris-EDTA buffer (10 mmol/L Tris [pH8.0], 1 mmol/L EDTA). Immunocomplexes were eluted from beads with 2 times 250 µl elution buffer (1% SDS, 0.1 mol/L NaHCO<sub>3</sub>) for 30 min at room temperature. Cross-links were reversed by addition of NaCl (0.3 mol/L final concentration) and RNA was removed by addition of RNase (10 µg/sample). The incubation was performed for 5 hours at 65°C. The DNA was precipitated with 2.5 Vol. 100% ethanol over night, resuspended in solution containing 40 mmol/L Tris [pH 6.5], 10 mmol/L EDTA, 20 µg proteinase K, and incubated for 2 hours at 45°C. The DNA was purified using QIAquick PCR purification kit (QIAGEN, no. 28106). The presence and quantities of genomic DNA specifying the promoter

regions of ANP, BNP and GAPDH were assessed by PCR. Primers are listed in Table S3,S4 and S5.

#### **cDNA from neuroblastoma- (SH-SY5Y) and kidney (293T) cells**

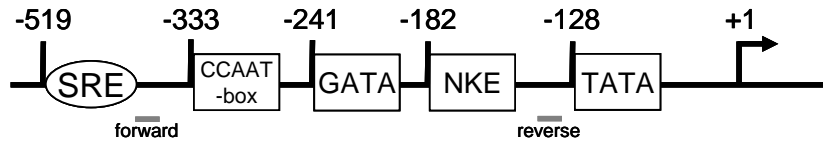
For experiments that investigated the regulation of REST in human myocardium, we used cDNA obtained from neuroblastoma- (SH-SY5Y) and kidney (293T) cells as controls.

#### **Working heart preparation and pressure volume measurements**

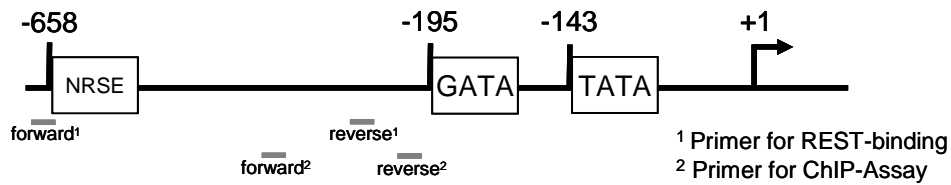
Studies on isolated working hearts were carried out as described previously (7). Mice were heparinized with 100 IU heparin 15 min prior to being killed by i.p. administration of pentobarbital-sodium (60mg/kg). The heart was excised and placed in ice-cold St. Thomas-Hospital solution (cardioplegia). Following removal of pericardium, lung and trachea, the aorta was cannulated with an 18-G metal cannula (1.5 cm of length; 0.95 mm inner diameter; 1.30 mm outer diameter) for a Langendorff retrograde perfusion (60mmHg perfusion pressure) with Krebs-Henseleit buffer (KHB) in a working heart apparatus (IH-SR Perfusion system type 844/1 Hugo Sachs Elektronik, Harvard Apparatus GmbH, March-Hugstetten, Germany). KHB (pH 7.4) comprised (in mM): NaCl 118.5, NaHCO<sub>3</sub> 25, KCl 4.7, MgSO<sub>4</sub> 1.2, KH<sub>2</sub>PO<sub>4</sub> 1.2, CaCl<sub>2</sub> 2.5, glucose 11.1, and was gassed with 95% O<sub>2</sub>, 5% CO<sub>2</sub>. Following establishment of coronary perfusion in the Langendorff mode, "working heart" preparation was continued by cannulating left atrium (LA) through the pulmonary vein with a 1.5 cm, 16-G steel cannula (1.14 mm inner diameter, 1.52 mm outer diameter) sewed in by a tobacco pouch suture (Ethicon Prolene 7.0). This cannula was connected to a preload column, which was water-jacketed and heated to 38°C, resulting in a myocardial temperature of 37°C when the heart was operating in the working mode (preload 10mmHg, afterload 80mmHg). Two platinum pacing electrodes embedded in polyester resin were attached to the right atrium to pace the hearts at 400 bpm. LV systolic and diastolic function was recorded via a high fidelity pressure catheter (Millar 1.4 F SPR-835, Millar, Houston, Texas) inserted into the LV cavity through a small hole in the apex made with a 22 1/4 gauge needle.

## Supplemental Figures

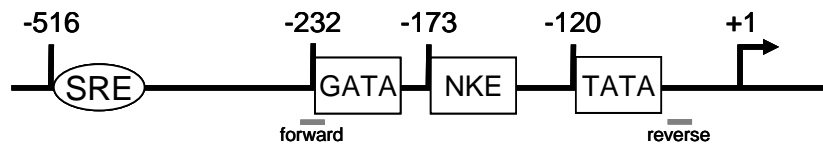
### A human ANP promoter



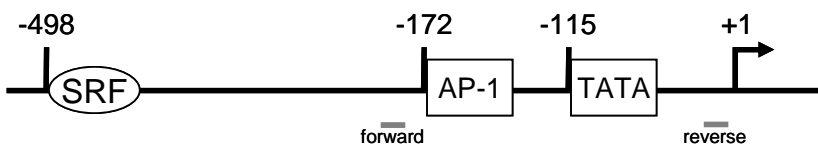
### B human BNP promoter



### C mouse ANP promoter



### D rat ANP promoter



### E rat BNP promoter

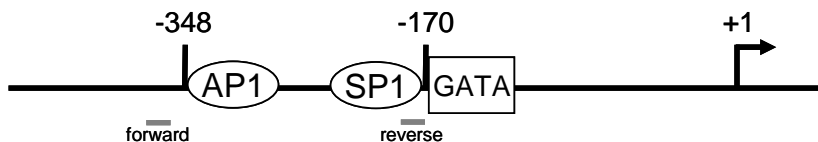


**Figure S1: Design of primers for ChIP of ANP and BNP promoter regions in human, mouse and rat myocardium.**

The forward and reverse primers for ChIP were designed to amplify comparable gene products in the vicinity of the TATA box in the promoter regions of ANP and BNP genes in human, mouse and rat myocardium, respectively (see tables 4 and 5 for primer sequences). Potential binding sites for transcription factors were searched by using "TFSEARCH: Searching Transcription Factor Binding Sites (ver 1.3)"

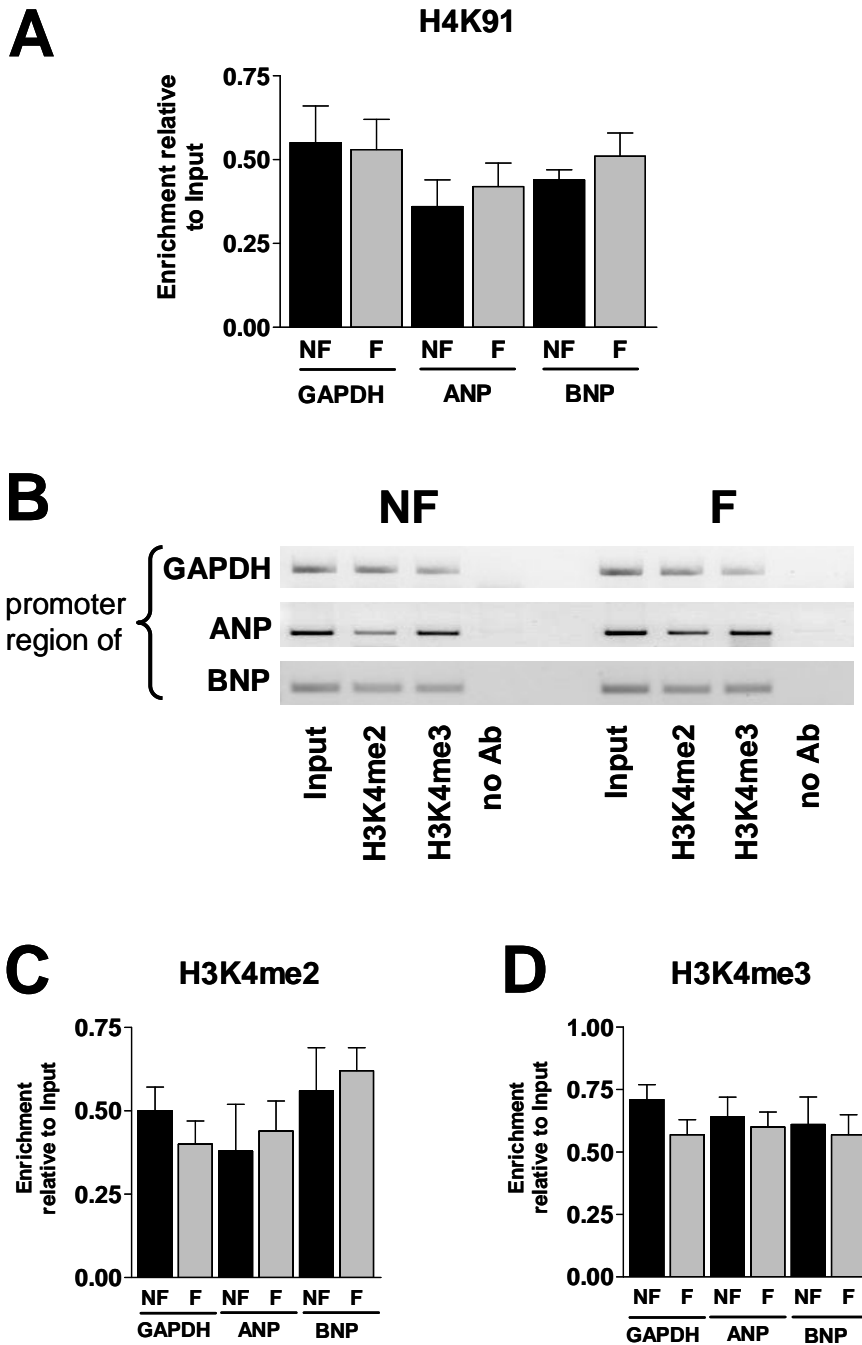


**Figure S2: Acetylation of H4K91 and methylation of H3K4 in failing and nonfailing myocardium**

**A**, Quantitative analysis of H4K91 acetylation determined by ChIP experiments on nonfailing (NF, n=8) and failing LV myocardium (F, n=16). Representative ChIP assay results (**B**) and cumulative analyses (**C-D**) for di- (me2) and trimethylated H3K4 (me3) in the promoter regions of ANP and BNP or NF and F myocardium. ChIP-assay experiments were performed at same time and under identical conditions.

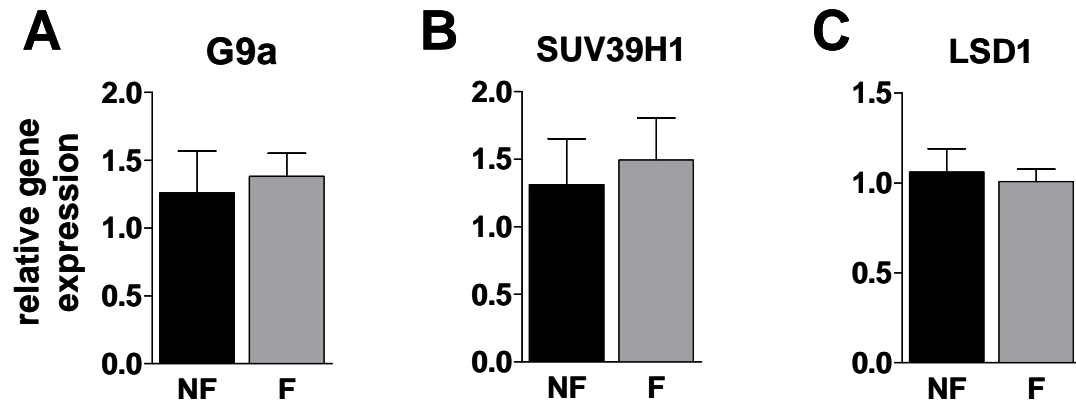


**Figure S3: Unchanged expression of histone methyltransferases and demethylases in human failing myocardium.** mRNA expression of G9a (A), SUV39H1 (B) and LSD1 (C) in human NF (n=8) and F myocardium (n=16).

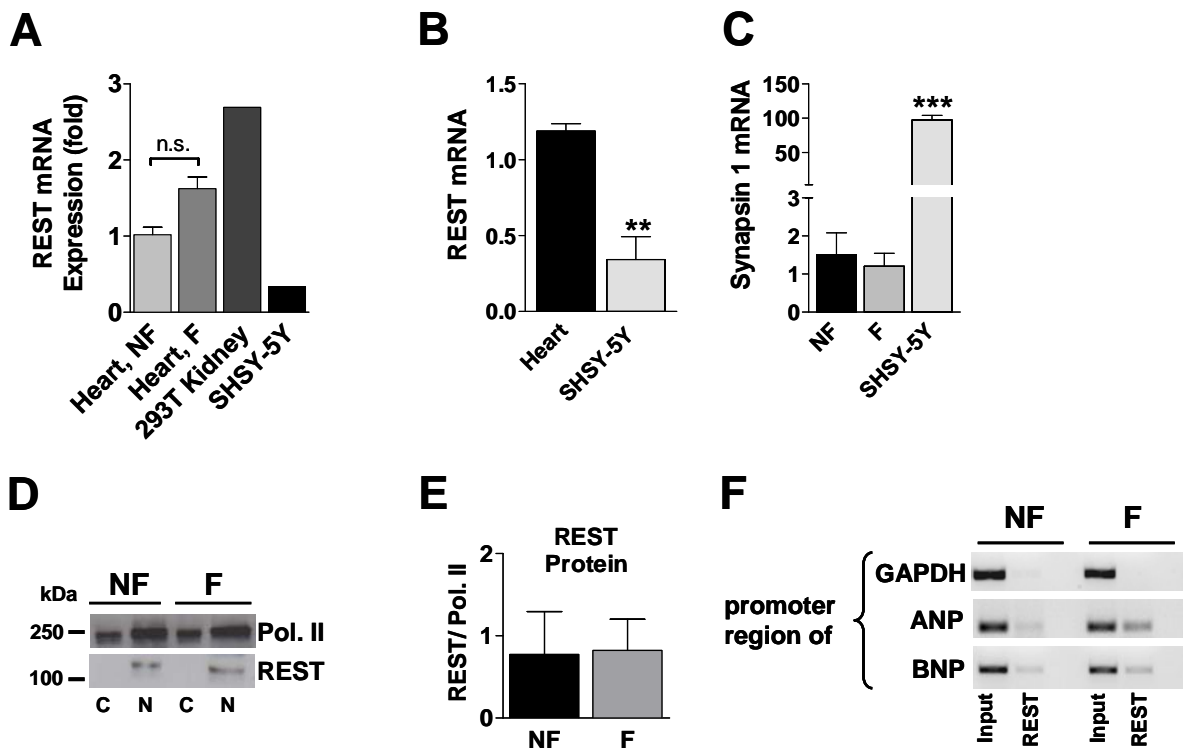


**Figure S4: Unchanged REST expression and recruitment to ANP and BNP promoter regions in human failing hearts.**

**A**, Quantitative real-time PCR analysis of REST gene expression in nonfailing (NF, n=8) and failing (F, n=16) myocardium. Human embryonic kidney cells (293T) and human neuroblastoma cells (SHSY-5Y) served as positive and negative controls, respectively. REST (**B**) and synapsin 1 mRNA expression (**C**) in human NF myocardium compared to SHSY-5Y neuroblastoma cells (n=5, respectively). Representative result of Western-blot analysis of REST in nuclear and cytosolic protein fractions of NF and F myocardium (**D**) and cumulative analysis of REST protein expression (**E**) in nuclear fractions of NF and F myocardium, normalized to polymerase II (Pol. II) expression, respectively. **F**, Recruitment of REST to promoter regions of ANP and BNP in NF and F myocardium, determined by ChIP analysis (representative of 2 experiments).



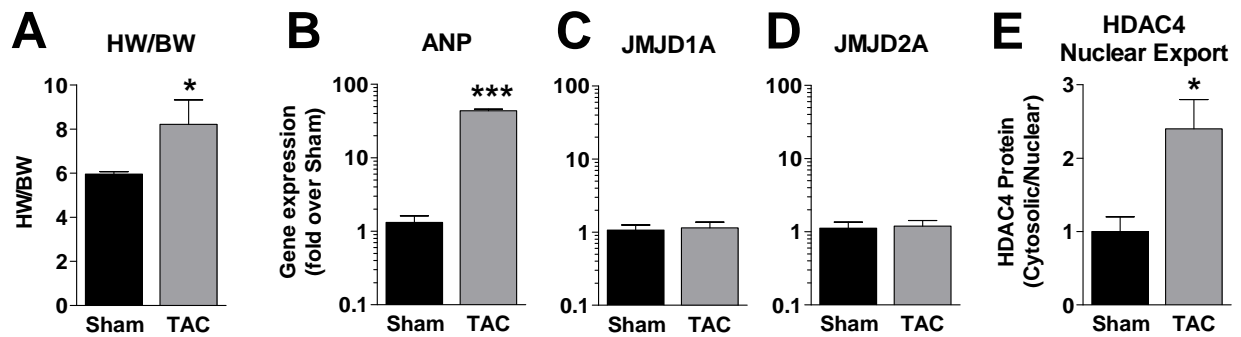


**Figure S5: JMJD1A and JMJD2A upregulation is not required for ANP upregulation in response to pressure overload.** Heart weight to body weight ratio (HW/BW; **A**), mRNA expression of ANP (**B**), JMJD1A (**C**) and JMJD2A (**D**) and nucleo-cytosolic shuttling of HDAC4, analyzed by Western blot analysis, in mouse hearts 6 weeks after TAC (n=4) or sham operation (Sham, n=4). \*p<0.05 and \*\*\*p<0.0001 vs. Sham.

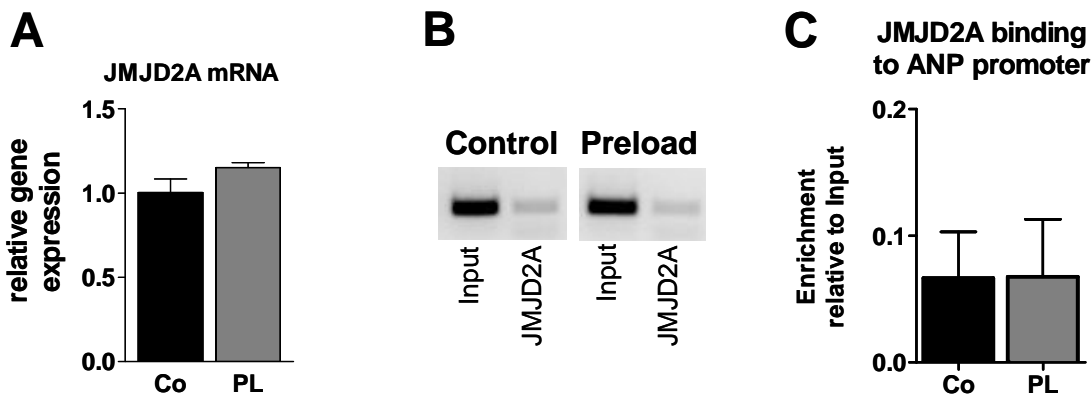


**Figure S6: Unchanged expression and binding activity of histone demethylase JMJD2A at the ANP promoter region in mouse hearts subjected to acutely elevated preload.**

Gene expression of JMJD2A in control (co) and preload (PL) hearts (**A**). Representative (**B**) and cumulative analysis (**C**) of ChIP-assay experiment probing for JMJD2A binding to the ANP promoter region.

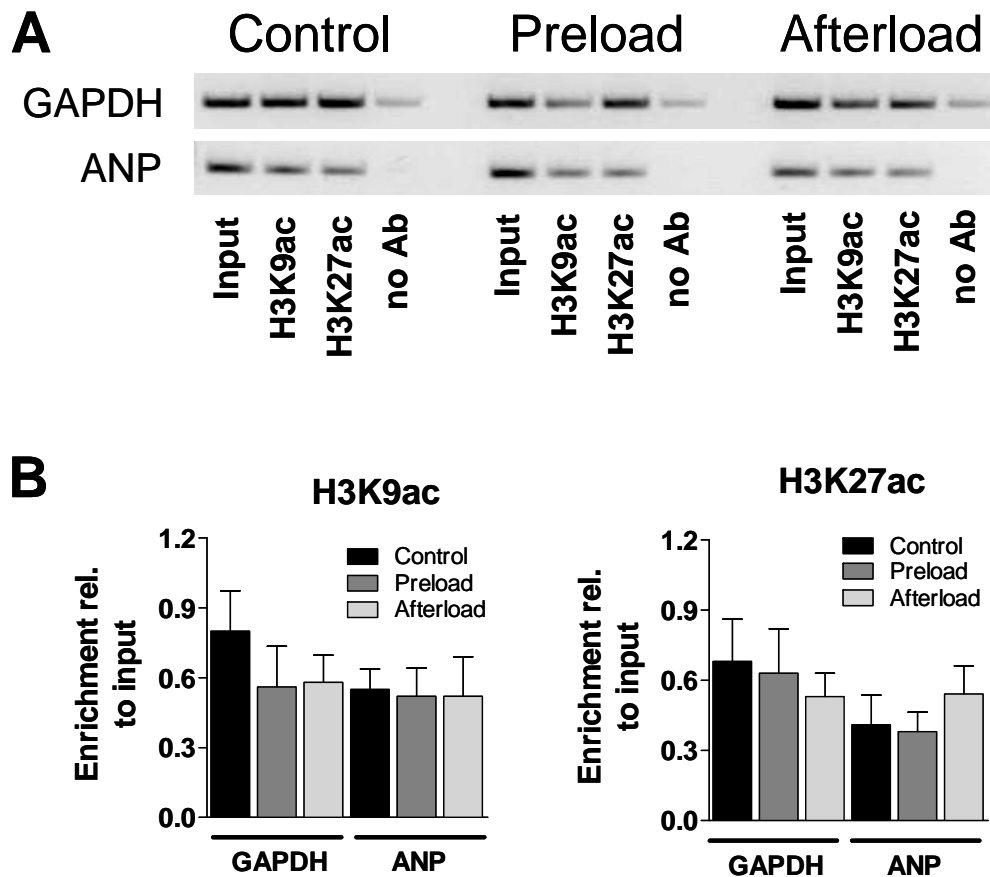


**Figure S7: Acutely increased cardiac load does not effect histone acetylation at the ANP promoter region.**

Representative (A) and cumulative analysis (B) of ChIP-assay experiments probing H3K9 and H3K27 acetylation (ac) in the promoter region of ANP in control-, preload- and afterload treated mouse hearts. ChIP-assay experiments were performed at same time and under identical conditions.

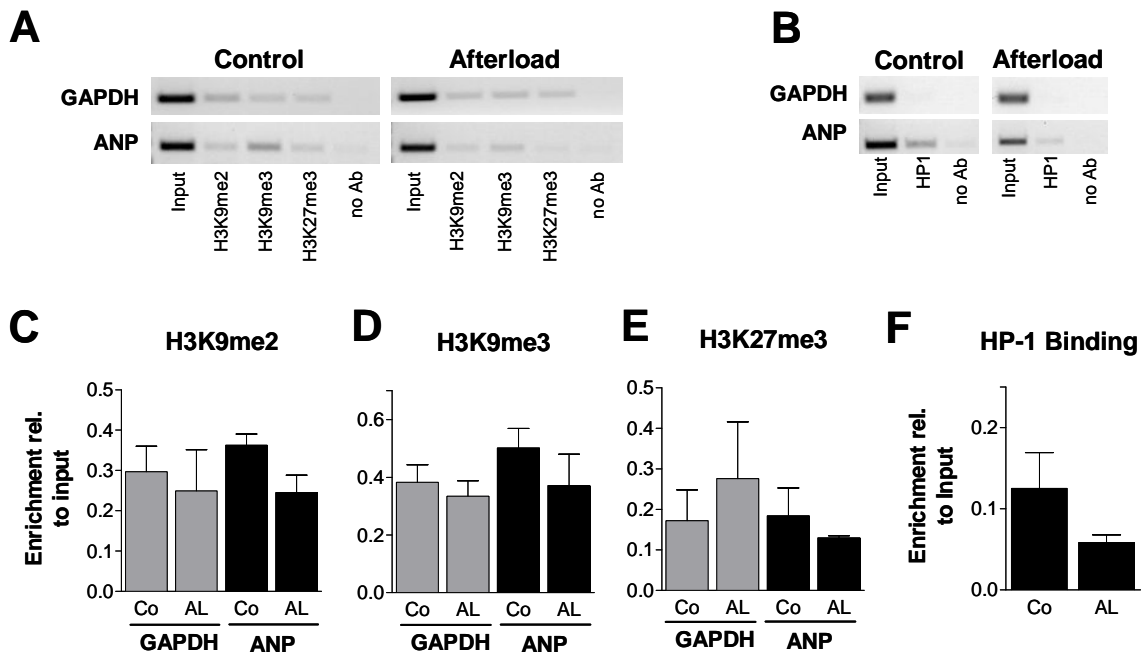


**Figure S8: Acutely increased afterload for 60 minutes did not result in a significant decrease of histone methylation and reduction of HP1 binding at the ANP promoter.** Representative ChIP-assay experiments probing di- (me2) and tri-methylated (me3) H3K9 and H3K27 (A) or HP1 binding (B) at the ANP promoter region (lanes were run on the same gel but were non-contiguous) and cumulative results (C-F) under 60 min of elevated afterload (AL) vs. control (Co) conditions. As a negative control, no antibody was added (no Ab). Input shows PCR product of total chromatin without prior IP.

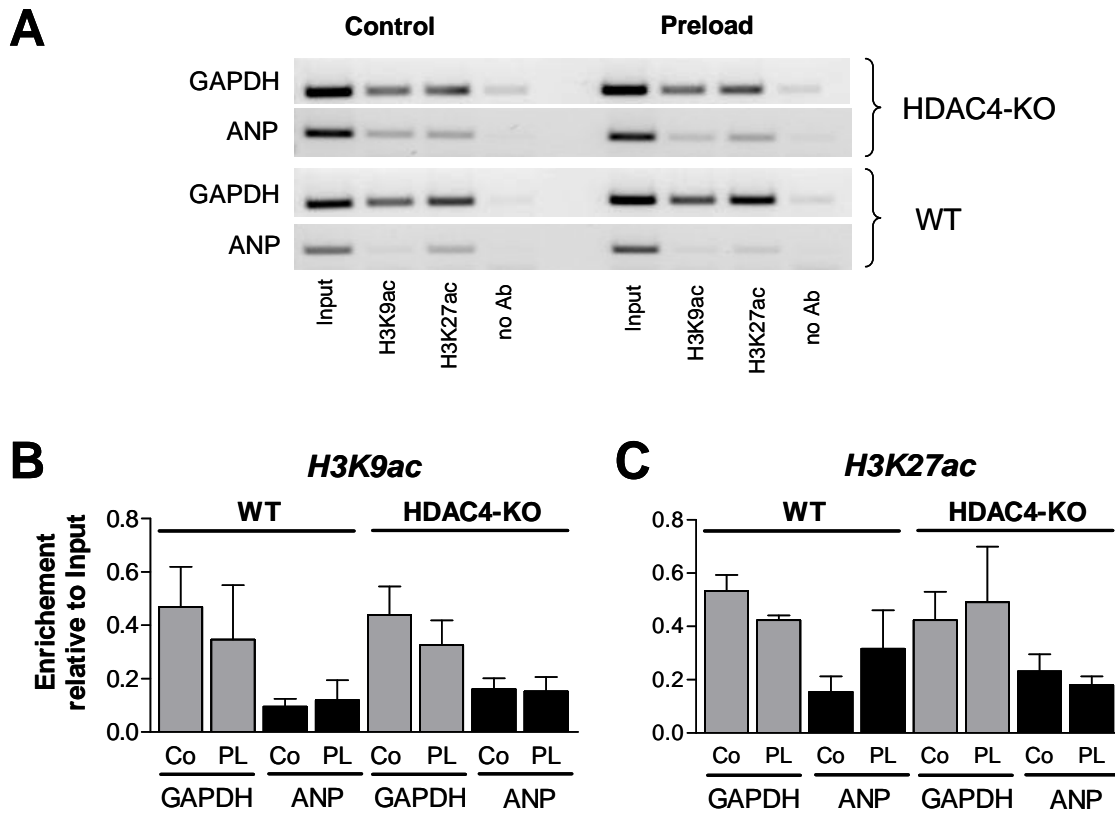


**Figure S9: Unchanged acetylation of H3K9 and H3K27 in WT and HDAC4-KO mice at physiological and elevated cardiac preload conditions.**

Representative results (A) and cumulative analysis (B, C) from ChIP experiments probing H3K9 and H3K27 acetylation in the promoter regions of ANP and GAPDH in WT and HDAC4-KO mice before and after elevation of cardiac preload from 10 to 30 mmHg, respectively. ChIP-assay experiments were performed at same time and under identical conditions.

## Supplemental Tables

**Table S1: Patient characteristics**

	NF	ICM	DCM
<b><i>Number of patients (n)</i></b>	8	8	8
Male / Female (n)	5/3	8/0	4/4
Age (years)	50±6	56±1	48±4
<b><i>Clinical parameters</i></b>			
NYHA class		3.3±0.2	3.6±0.2
LVEF (%)		24±3	14±2
PCWP (mmHg)		27±3	24±3
C.I. (mL/min*m <sup>2</sup> )		2.1±0.2	1.8±0.3
LVEDD (mm)		69±3	70±5
FS (%)		15±1	13±2
<b><i>Medication</i></b>			
ACE-I/ AT <sub>1</sub> -Ant		88%	75%
β-Blockers		75%	50%
Aldosterone-Ant		50%	63%
Digitalis		38%	25%
Diuretics		88 %	100%
Inotropes		50%	38%
Nitrates		50%	0%
Statins		75%	0%

**Table S2: Forward and reverse primers for real-time PCR experiments (human)**

<b>Gene</b>	<b>Forward Primer</b>	<b>Reverse Primer</b>
<b>ANP</b>	GAT AAC AGC CAG GGA GGA CA	ATC ACA ACT CCA TGG GAA CA
<b>BNP</b>	TTC TTG CAT CTG GCT TTC CT	AGG GAT GTC TGC TCC ACC
<b>REST</b>	GAA TCT GGC TCT TCC ACT GC	GTG TGG TGT TTC AGG TGT GC
<b><math>\alpha</math>MHC</b>	GAA AAA GGG CTC ATC CTT CC	GAT GAT GCA ACG CAC AAA GT
<b>Serca2A</b>	ACC CAC ATT CGA GTT GGA AG	CAG TGG GTT GTC ATG AGT GG
<b>GAPDH</b>	ATG ACA TCA AGA AGG TGG TG	CAT ACC AGG AAA TGA GCT TG
<b>JMJD1A</b>	GAG CTG TTT CCC ACA CCG A	TGC TCT CCT TAG AAG GCT GTA GAC
<b>JMJD2A</b>	CGA GAG TTC CGC AAG ATA GC	CTC CTT TTC CAC CAA GTC CA
<b>JMJD2B</b>	GGG GAG GAA GAT GTG AGT GA	GAC GGC TTT TGG AGG GTA AT
<b>G9a</b>	TGA CTG CGT GCT GTT ATT CC	TGA TCT TCT CTG TGC GGA TG
<b>LSD1</b>	ATC TGC AGT CCA AAG GAT GG	GCC AAC AAT CAC ATC GTC AC
<b>SUV39H1</b>	GGC AAC ATC TCC CAC TTT GT	CAA TAC GGA CCC GCT TCT TA
<b>Synapsin 1</b>	AAT ACT GGC TCT GCG ATG CT	TGT CTT CAT CCT GGT GGT CA

**Table S3: TaqMan probes (Applied Biosystems) for TaqMan PCR experiments**

<b>Gene</b>	<b>Probe number</b>
<b>Nppa (mouse)</b>	Mm01255770_g1
<b>GAPDH (mouse)</b>	Mm99999915_g1
<b>Nppa (rat)</b>	Rn00561661_m1
<b>Nppb (rat)</b>	Rn00676450_g1
<b>Jmjd1a (rat)</b>	Rn00598469_m1
<b>Jmjd2a (rat)</b>	Rn01417083_m1
<b>Serca2a (rat)</b>	Rn00568762_m1
<b>Suv39H1 (rat)</b>	Rn01528295_m1
<b>FHL1 (rat)</b>	Rn01402101_m1
<b>GAPDH (rat)</b>	Rn99999916_s1

**Table S4: Forward and reverse primers for 5' promoter regions of genes in ChIP assays (human)**

<b>Gene (<i>human</i>)</b>	<b>Forward Primer</b>	<b>Reverse Primer</b>
<b>ANP</b>	GAC AGC TGA GCC ACA AAC AA	AGT GAG AAG CCA GCA GGA GA
<b>ANP -REST binding-</b>	GAT AAC AGC CAG GGA GGA CA	ATC ACA ACT CCA TGG CAA CA
<b>BNP</b>	GGC TGT TTT CGC TGT GAG TC	TTC CTT TCC TGC AAA TGT CC
<b>BNP -REST binding-</b>	CCT GAA AAT CCC GTT GAA GA	TGA CTC ACA GCG AAA ACA GC
<b>GAPDH</b>	CCC AAA GTC CTC CTG TTT CA	GTC TTG AGG CCT GAG CTA CG

**Table S5: Forward and reverse primers for 5' promoter regions of genes in ChIP assays (mouse)**

<b>Gene (<i>mouse</i>)</b>	<b>Forward Primer</b>	<b>Reverse Primer</b>
<b>ANP</b>	ACA AGC TTT GCC GAA CTG AT	TCA GCT TTT GTC CGT CAC TG
<b>GAPDH</b>	AGG AGA AAG TGG GGA AAA GC	GCC TTG CAG AAA CTT TGG AG

**Table S6: Forward and reverse primers for 5' promoter regions of genes in ChIP assays (rat)**

<b>Gene (<i>rat</i>)</b>	<b>Forward Primer</b>	<b>Reverse Primer</b>
<b>ANP</b>	ACAAGCTTCGCTGGACTGAT	GCTGTCTCGGCTCACTCTCT
<b>BNP</b>	GAGCAGGAAACAAGGACCTG	GGGTGGGGTTATCTCTGAT

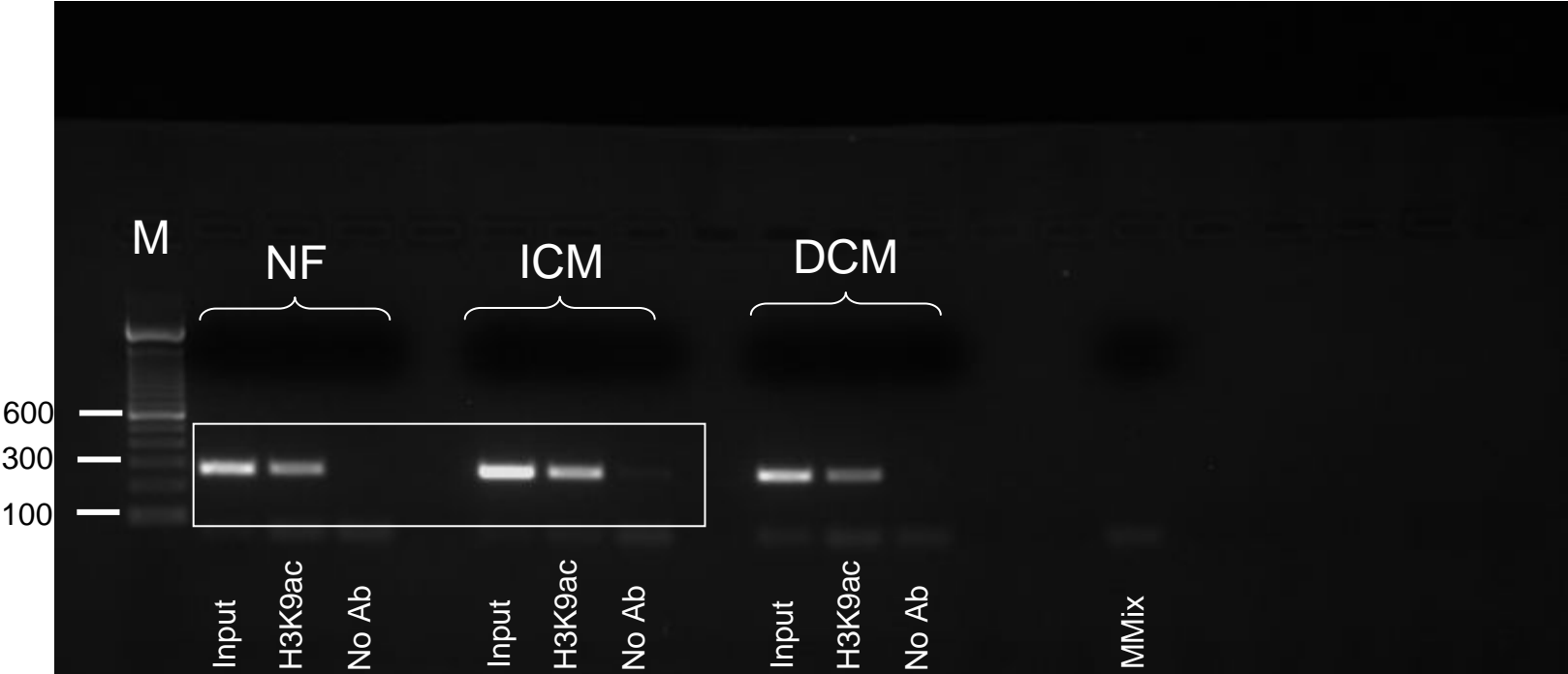


## Supplemental References

1. Chong, J.A., Tapia-Ramirez, J., Kim, S., Toledo-Aral, J.J., Zheng, Y., Boutros, M.C., Altshuler, Y.M., Frohman, M.A., Kraner, S.D., and Mandel, G. 1995. REST: a mammalian silencer protein that restricts sodium channel gene expression to neurons. *Cell* 80:949-957.
2. Ballas, N., Grunseich, C., Lu, D.D., Speh, J.C., and Mandel, G. 2005. REST and its corepressors mediate plasticity of neuronal gene chromatin throughout neurogenesis. *Cell* 121:645-657.
3. Kuwahara, K., Saito, Y., Ogawa, E., Takahashi, N., Nakagawa, Y., Naruse, Y., Harada, M., Hamanaka, I., Izumi, T., Miyamoto, Y., et al. 2001. The neuron-restrictive silencer element-neuron-restrictive silencer factor system regulates basal and endothelin 1-inducible atrial natriuretic peptide gene expression in ventricular myocytes. *Mol Cell Biol* 21:2085-2097.
4. Kuwahara, K., Saito, Y., Takano, M., Arai, Y., Yasuno, S., Nakagawa, Y., Takahashi, N., Adachi, Y., Takemura, G., Horie, M., et al. 2003. NRSF regulates the fetal cardiac gene program and maintains normal cardiac structure and function. *Embo J* 22:6310-6321.
5. Nakagawa, Y., Kuwahara, K., Harada, M., Takahashi, N., Yasuno, S., Adachi, Y., Kawakami, R., Nakanishi, M., Tanimoto, K., Usami, S., et al. 2006. Class II HDACs mediate CaMK-dependent signaling to NRSF in ventricular myocytes. *J Mol Cell Cardiol* 41:1010-1022.
6. Ooi, L., and Wood, I.C. 2007. Chromatin crosstalk in development and disease: lessons from REST. *Nat Rev Genet* 8:544-554.
7. Bingham, A.J., Ooi, L., Kozera, L., White, E., and Wood, I.C. 2007. The repressor element 1-silencing transcription factor regulates heart-specific gene expression using multiple chromatin-modifying complexes. *Mol Cell Biol* 27:4082-4092.
8. Belyaev, N.D., Wood, I.C., Bruce, A.W., Street, M., Trinh, J.B., and Buckley, N.J. 2004. Distinct RE-1 silencing transcription factor-containing complexes interact with different target genes. *J Biol Chem* 279:556-561.
9. Toischer, K., Rokita, A.G., Unsöld, B., Zhu, W., Kararigas, G., Sossalla, S., Reuter, S.P., Becker, A., Teucher, N., Seidler, T., et al. 2010. Differential cardiac remodeling in preload versus afterload. *Circulation* 122:993-1003.
10. Toischer, K., Teucher, N., Unsöld, B., Kuhn, M., Kögler, H., and Hasenfuss, G. BNP controls early load-dependent regulation of SERCA through calcineurin. *Basic Res Cardiol* 105:795-804.
11. Reil, J.C., Hohl, M., and Böhm, M. Letter by Reil et al regarding article, "Differential cardiac remodeling in preload versus afterload". *Circulation* 123:e420; author reply e421.
12. Livak, K.J., and Schmittgen, T.D. 2001. Analysis of relative gene expression data using real-time quantitative PCR and the 2(-Delta Delta C(T)) Method. *Methods* 25:402-408.

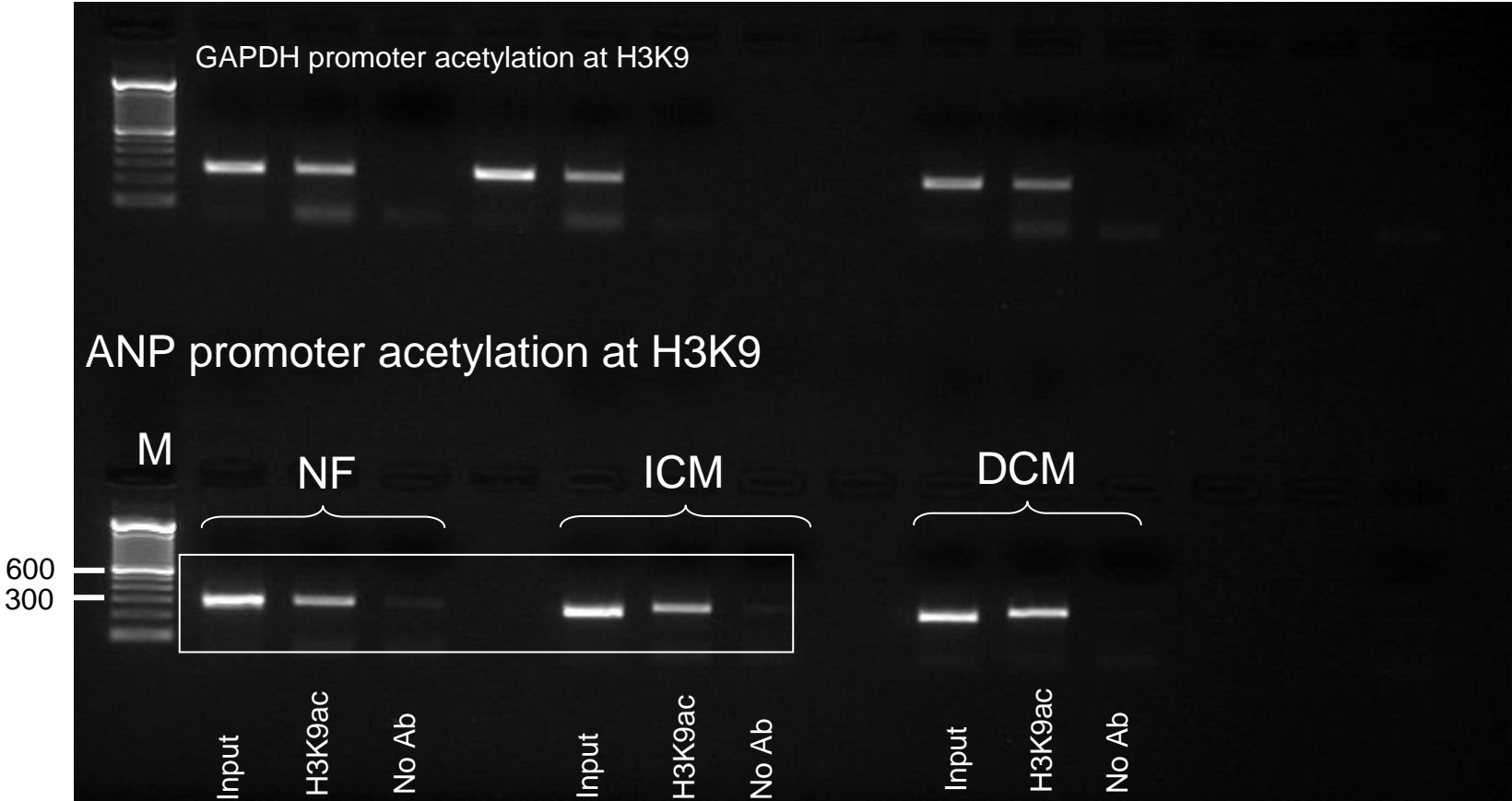
Full unedited gels for Figure 2A

GAPDH promoter acetylation at H3K9



M = 100bp DNA Ladder (Invitrogen)  
2% Agarose gel  
PCR product for GAPDH-promoter : 262bp

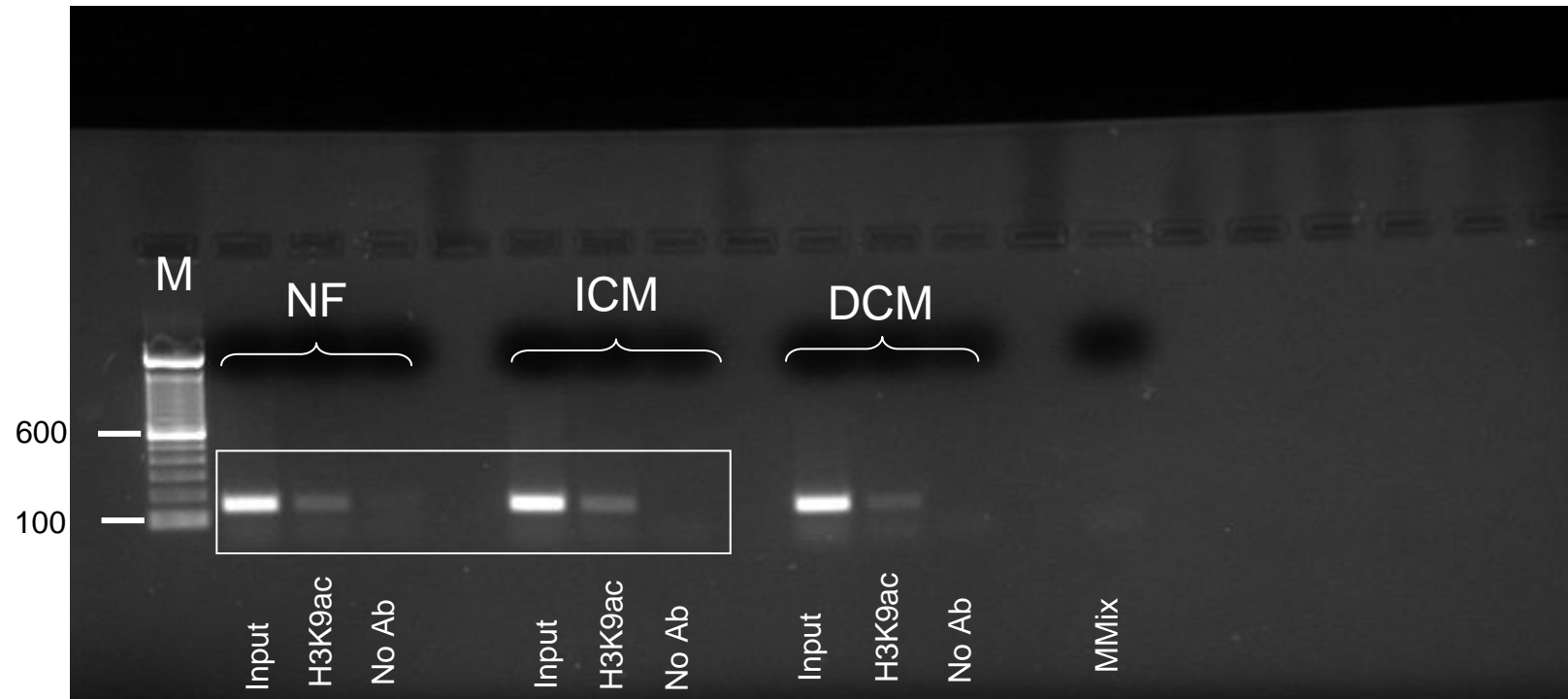
Full unedited gels for Figure 2A



M = 100bp DNA Ladder (Invitrogen)  
2% Agarose gel  
PCR product for ANP-promoter : 299bp

# Full unedited gels for Figure 2A

## BNP promoter acetylation at H3K9



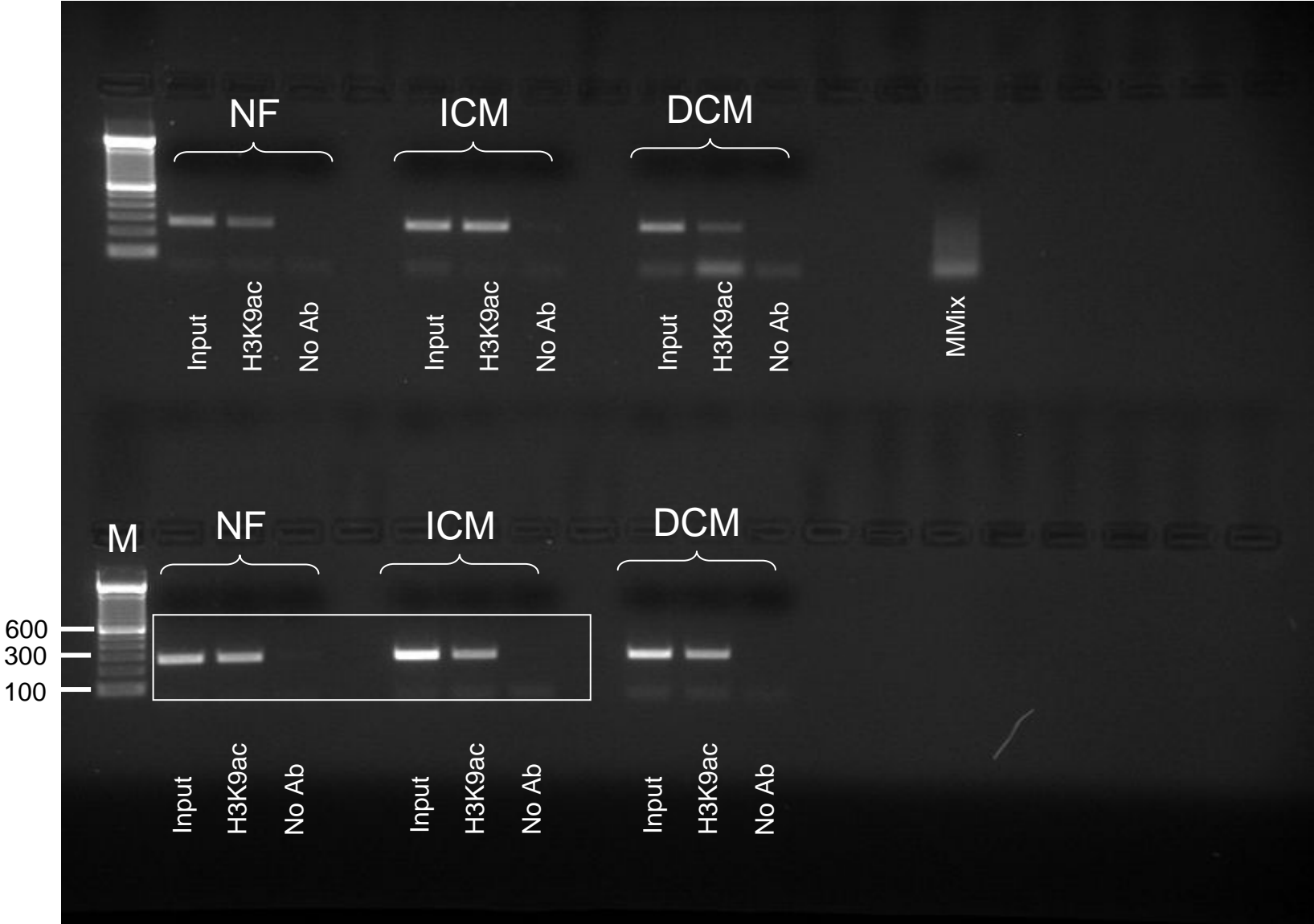
M = 100bp DNA Ladder (Invitrogen)

2% Agarose gel

PCR product for BNP-promoter : 150bp

Full unedited gels for Figure 2C

GAPDH promoter acetylation at H3K27

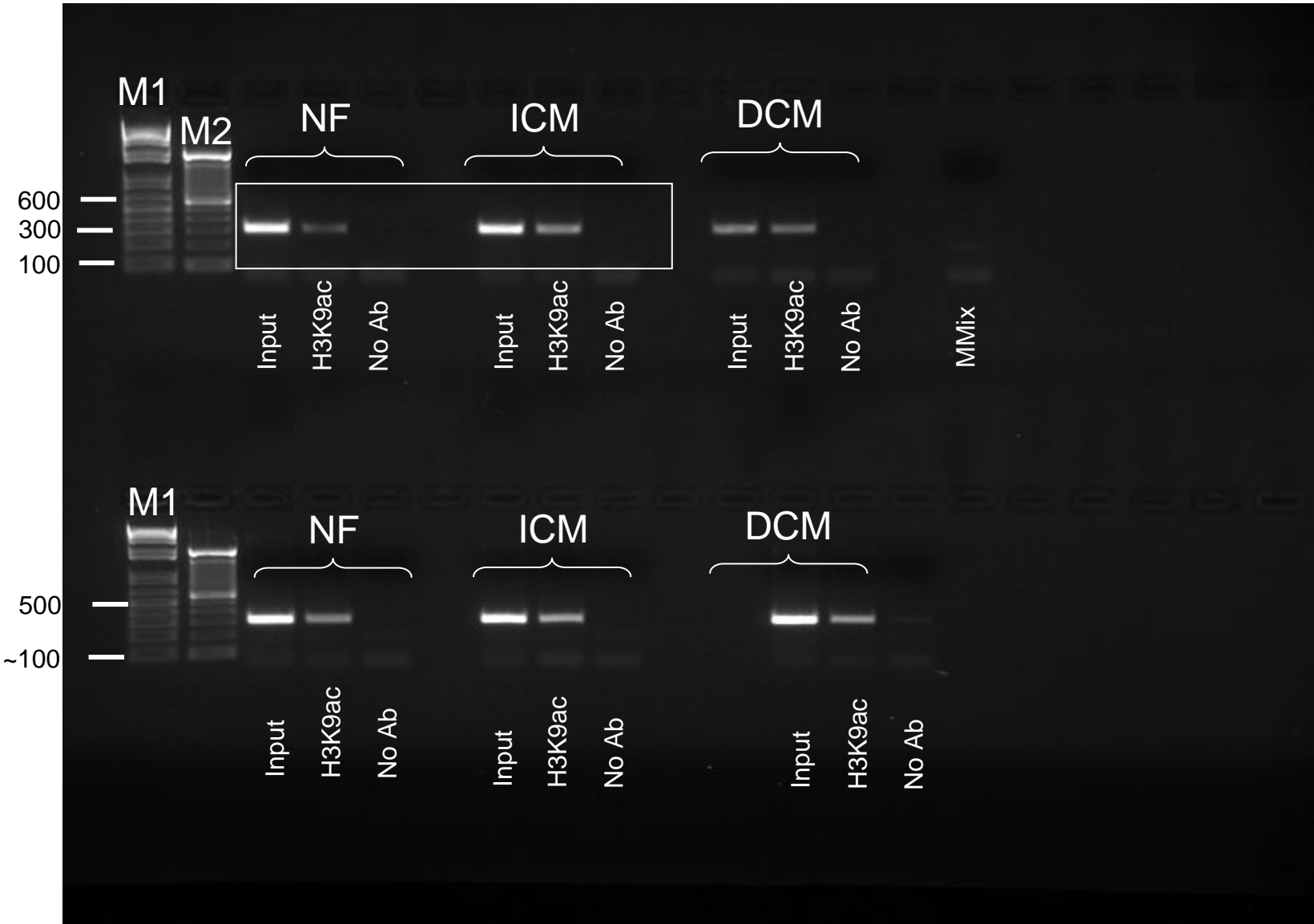


2% Agarose gel  
PCR product for GAPDH-promoter : 262bp

M = 100bp DNA Ladder (Invitrogen)

Full unedited gels for Figure 2C

ANP promoter acetylation at H3K27

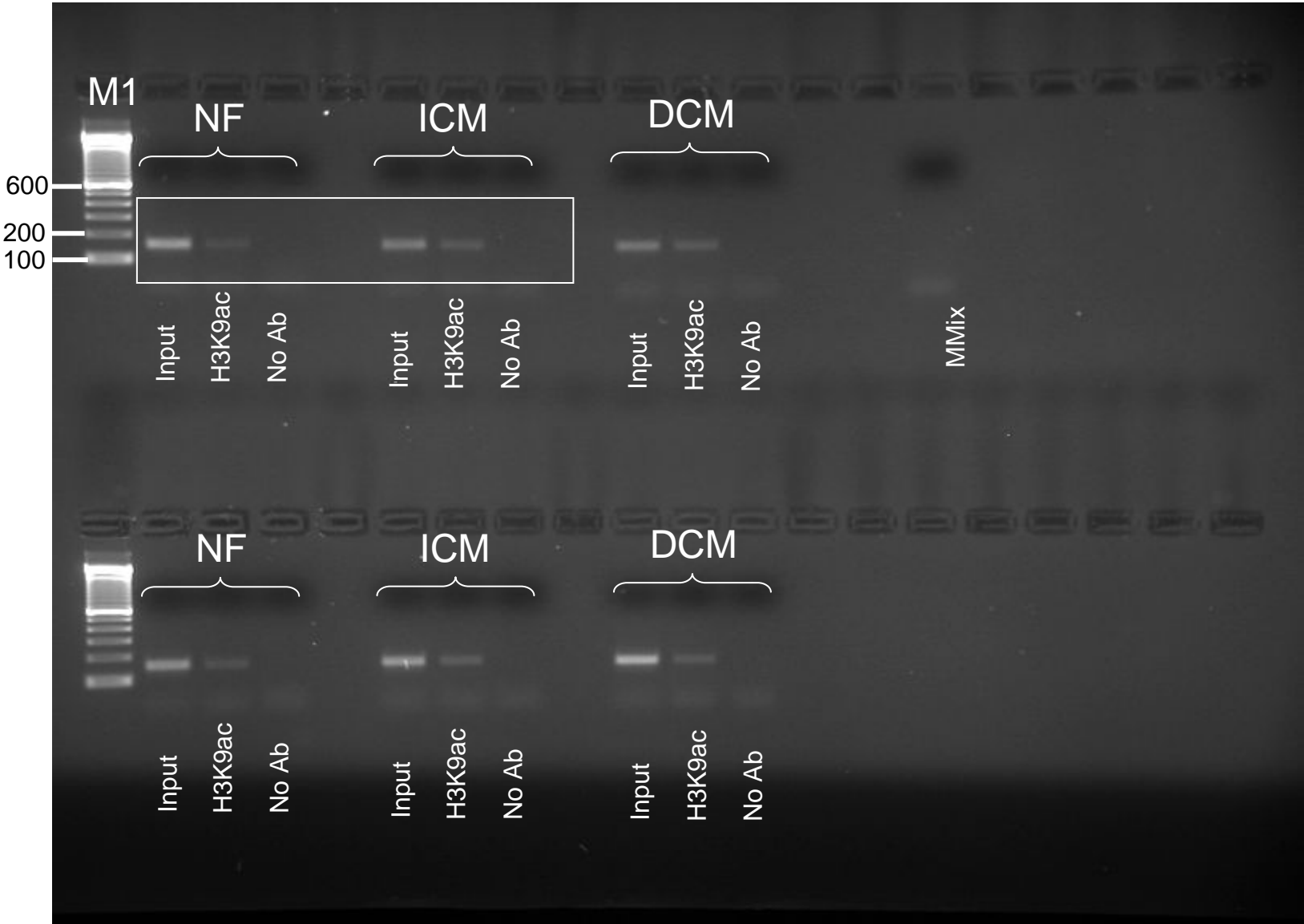


2% Agarose gel  
PCR product for ANP-promoter : 299bp

M1 = 1 kb DNA Ladder (Invitrogen)  
M2 = 100bp DNA Ladder (Invitrogen)

Full unedited gels for Figure 2C

BNP promoter acetylation at H3K27

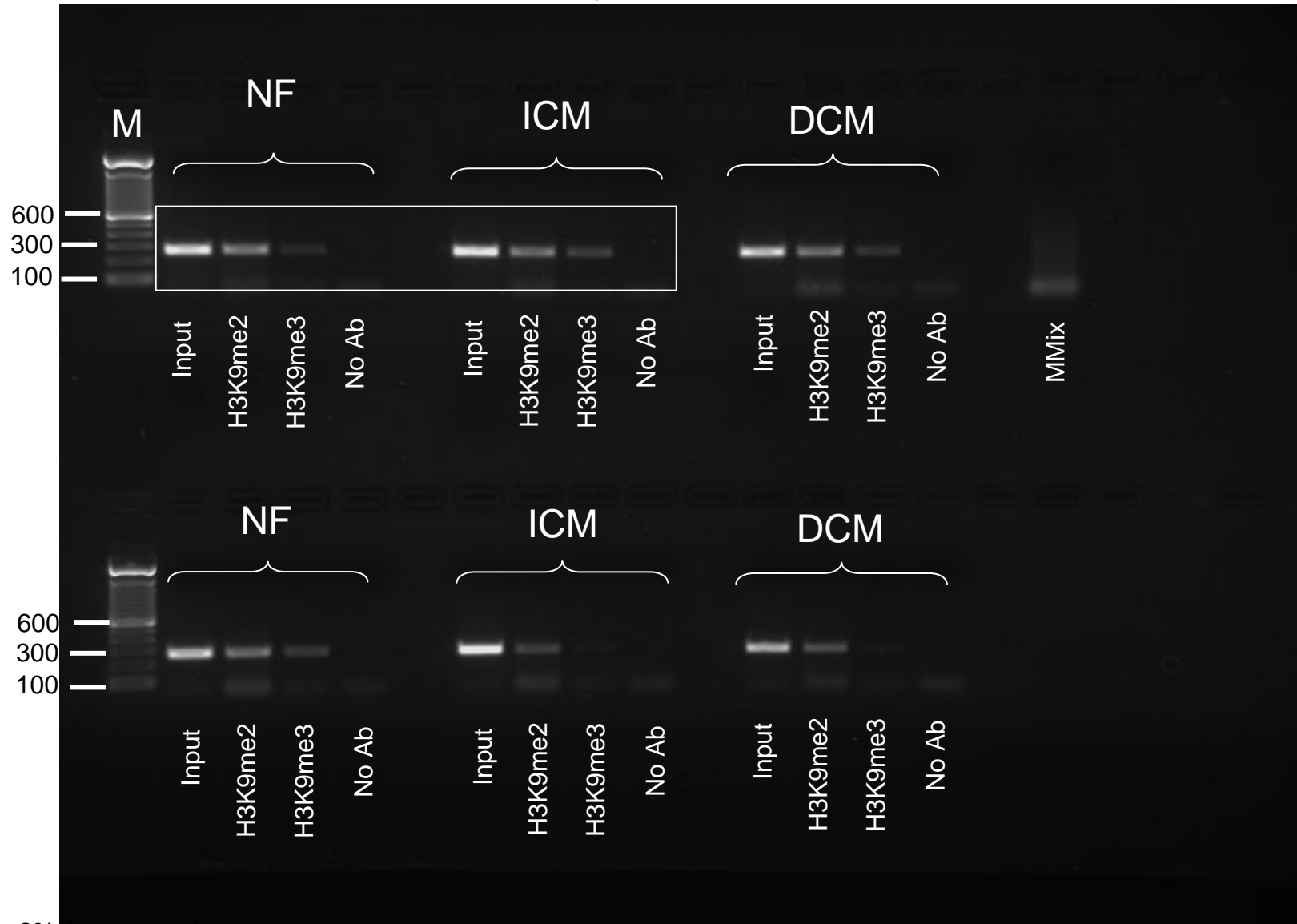


2% Agarose gel  
PCR product for BNP-promoter : 150bp

M= 100bp DNA Ladder (Invitrogen)

# Full unedited gel for Figure 3A

## Human GAPDH promoter methylation at H3K9



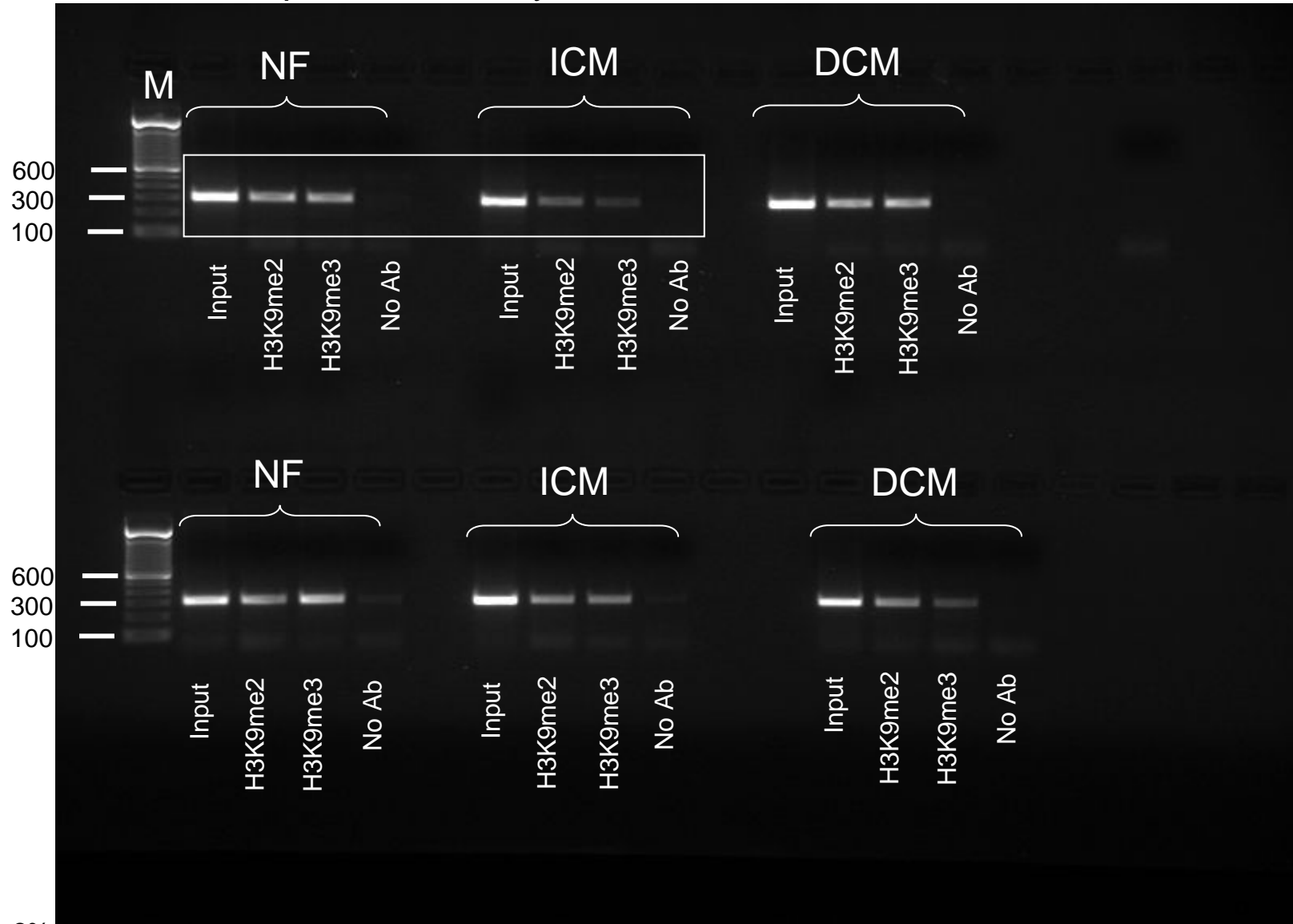
2% Agarose gel  
PCR product for GAPDH-promoter : 262bp

M = 100bp DNA Ladder (Invitrogen)



# Full unedited gel for Figure 3A

## Human ANP promoter methylation at H3K9

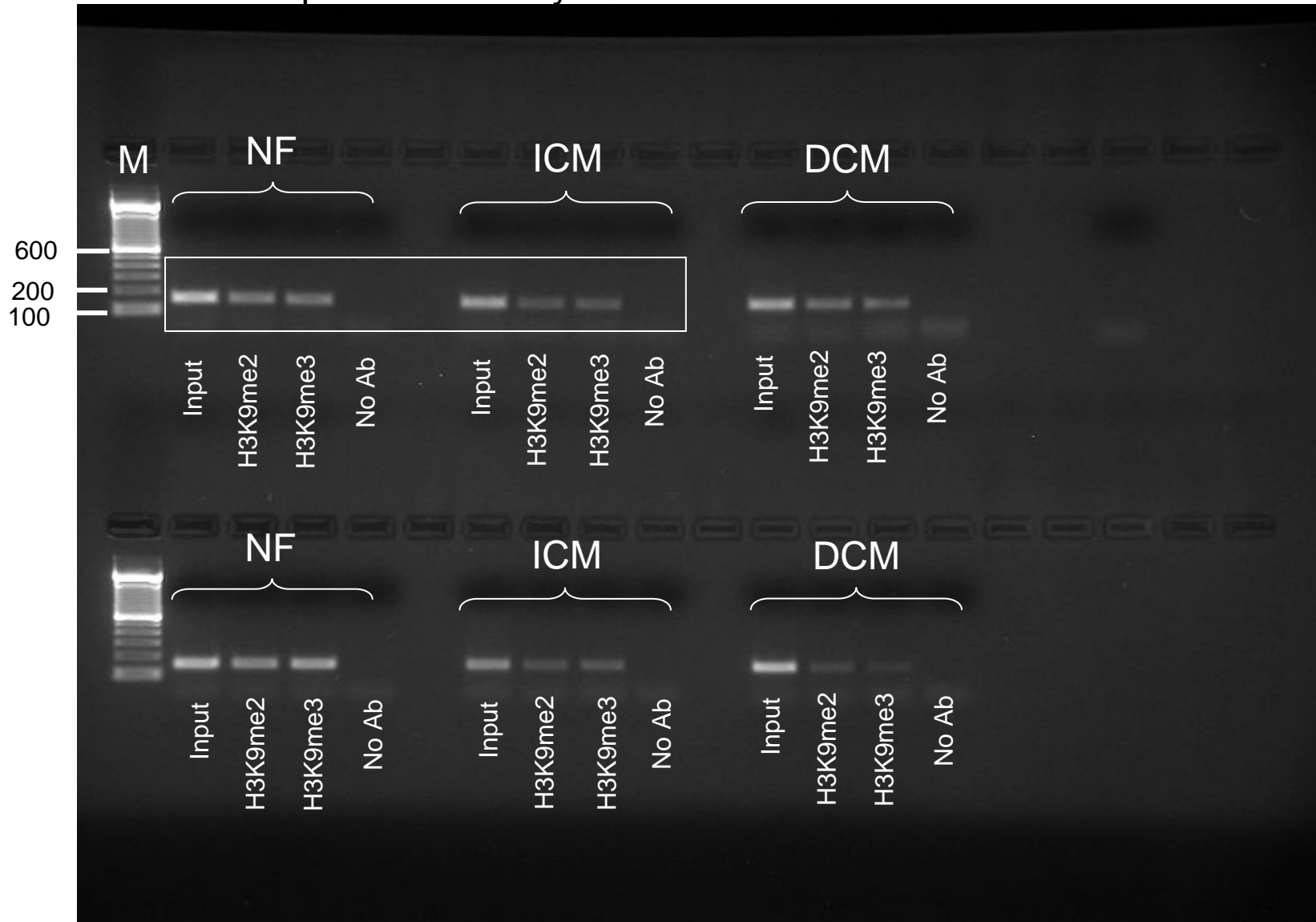


2% Agarose gel  
PCR product for ANP-promoter : 299bp

M = 100bp DNA Ladder (Invitrogen)

# Full unedited gel for Figure 3A

## Human BNP promoter methylation at H3K9

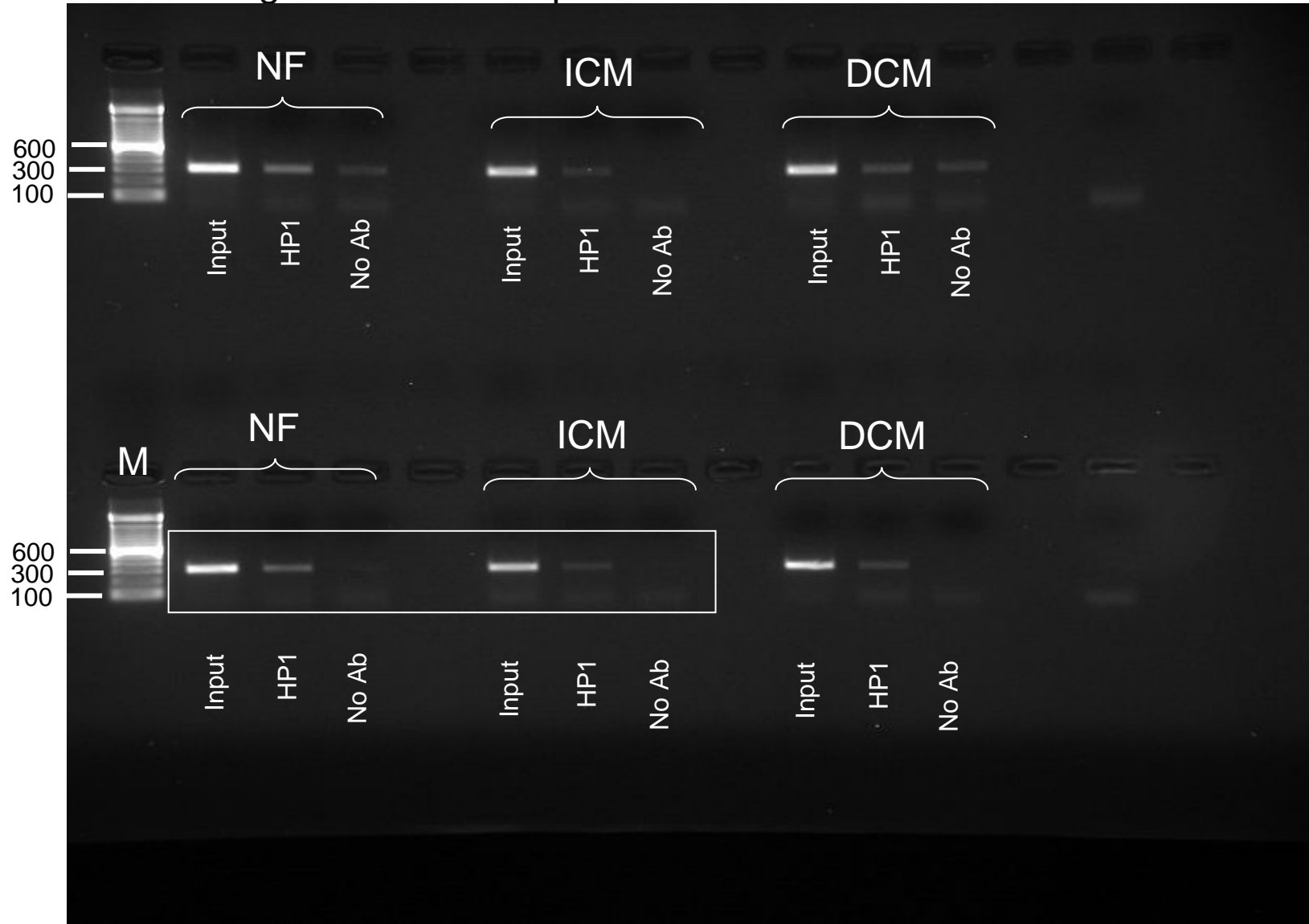


2% Agarose gel  
PCR product for BNP-promoter : 150bp

M = 100bp DNA Ladder (Invitrogen)

# Full unedited gel for Figure 3D

## HP1 Binding at human ANP promoter

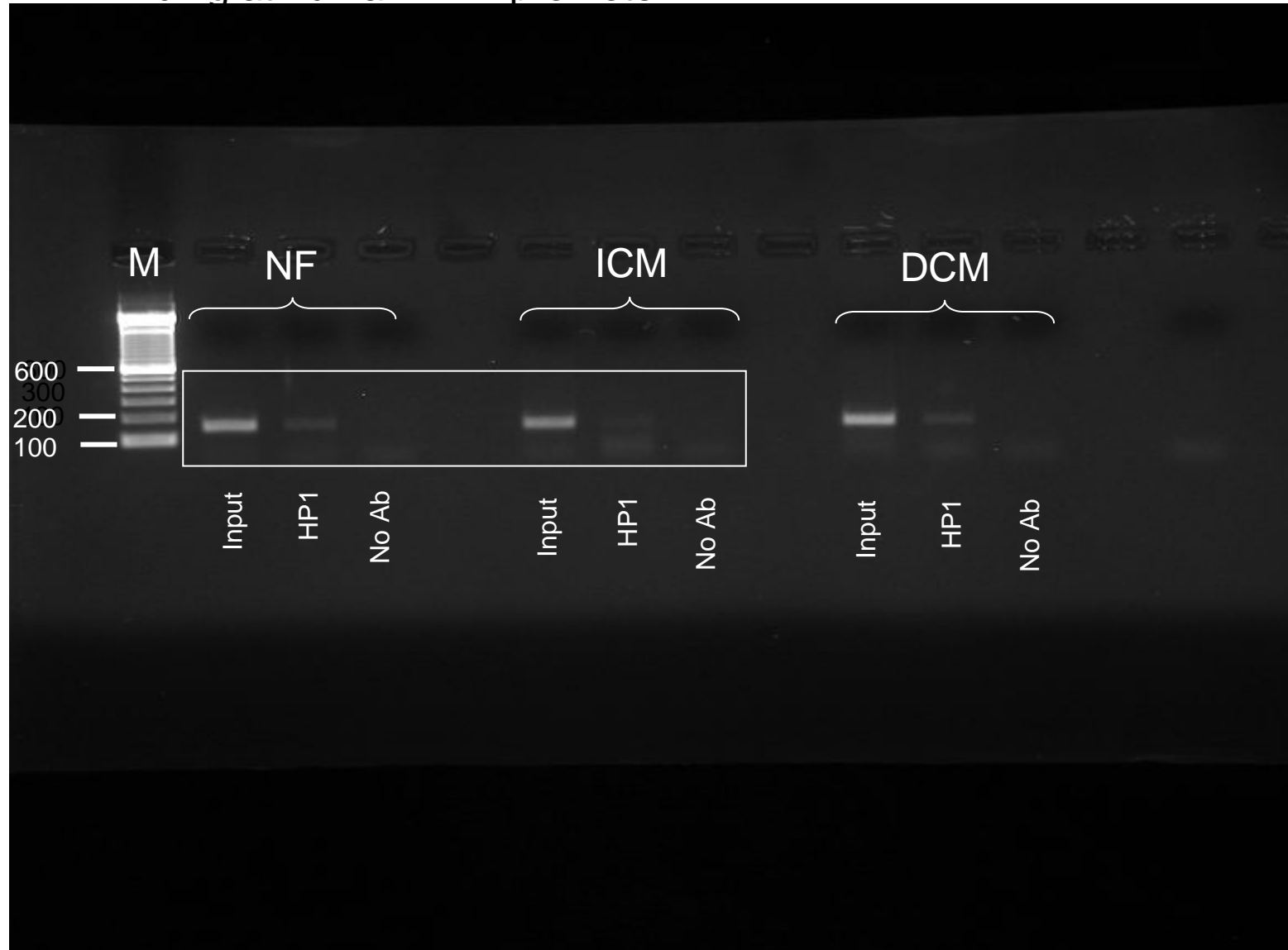


2% Agarose gel  
PCR product for ANP-promoter : 299bp

M = 100bp DNA Ladder (Invitrogen)

# Full unedited gel for Figure 3D

## HP1 Binding at human BNP promoter

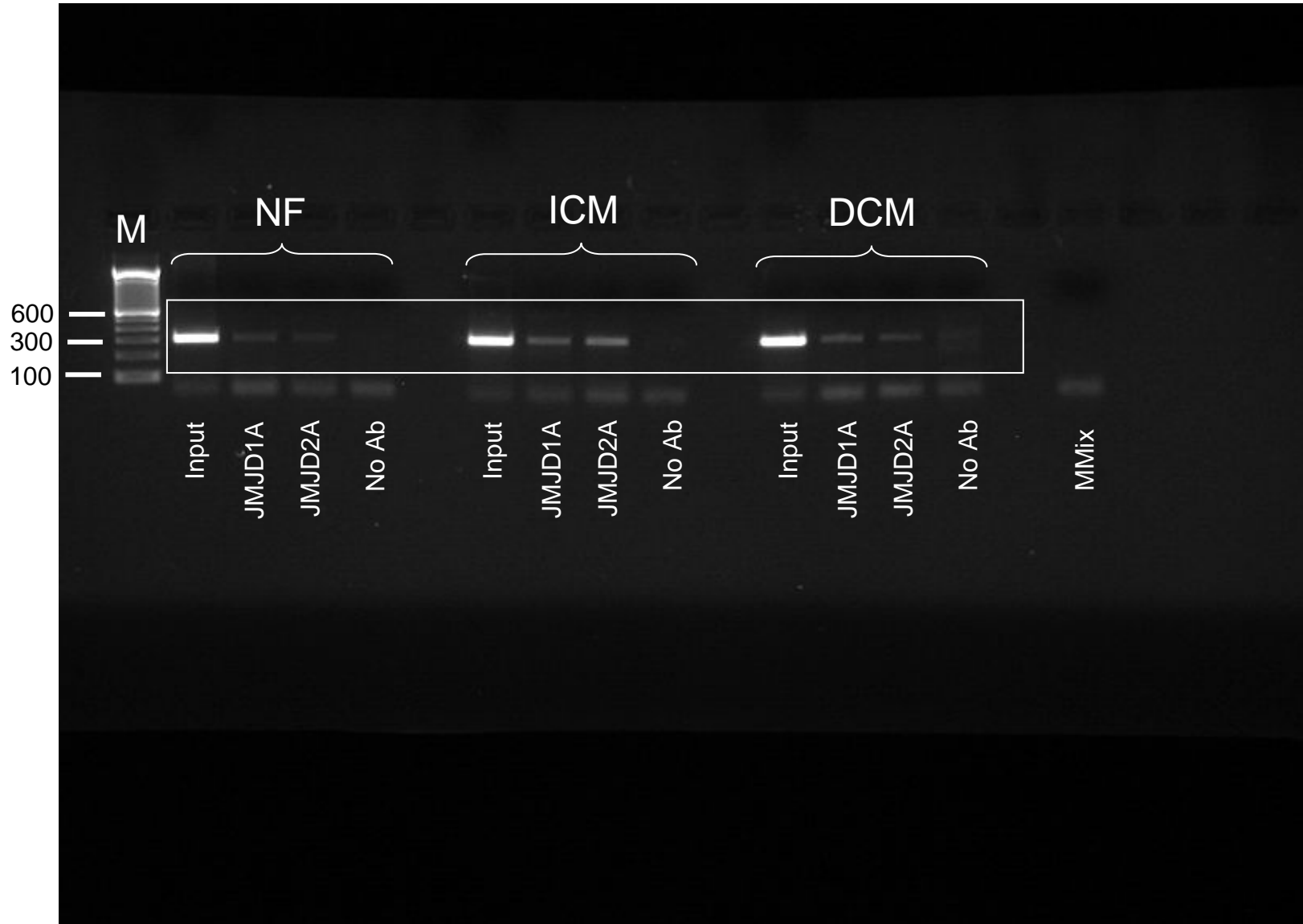


2% Agarose gel  
PCR product for BNP-promoter : 150bp

M = 100bp DNA Ladder (Invitrogen)

# Full unedited gel for Figure 4

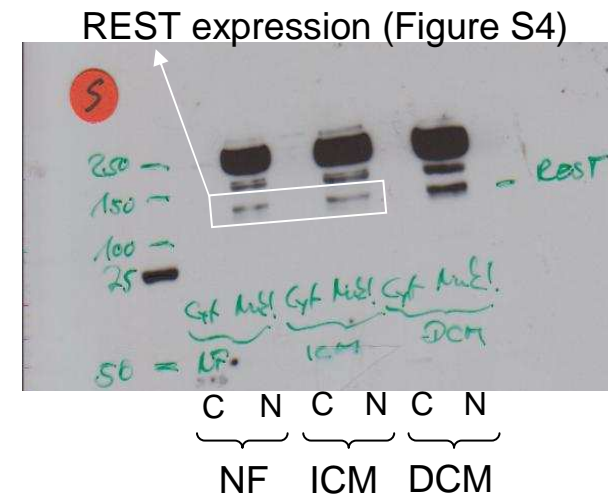
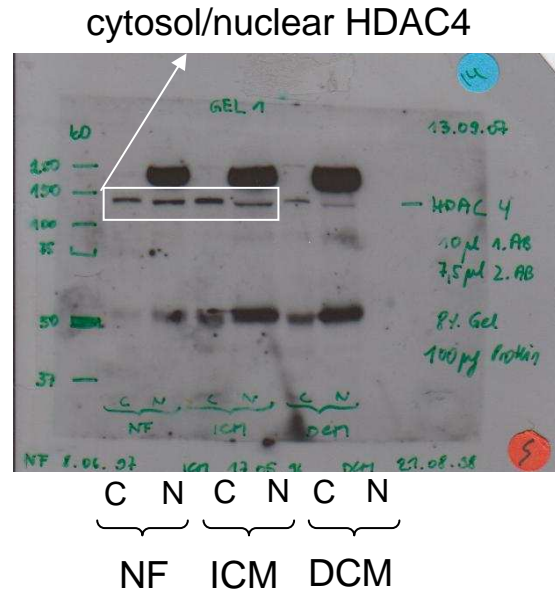
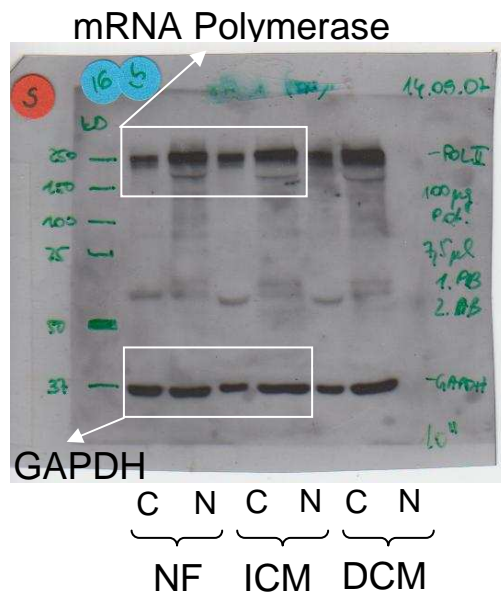
## JMJD1A and JMJD2A binding at human ANP promoter



2% Agarose gel  
PCR product for ANP-promoter : 299bp

M = 100bp DNA Ladder (Invitrogen)

# Full unedited gels Figure 5



C= cytosolic protein fraction  
N= nuclear protein fraction

# Full unedited gel for Figure 6F

Rat ANP promoter methylation  
JMJD1/2 double knock down: siScr and siJMJD



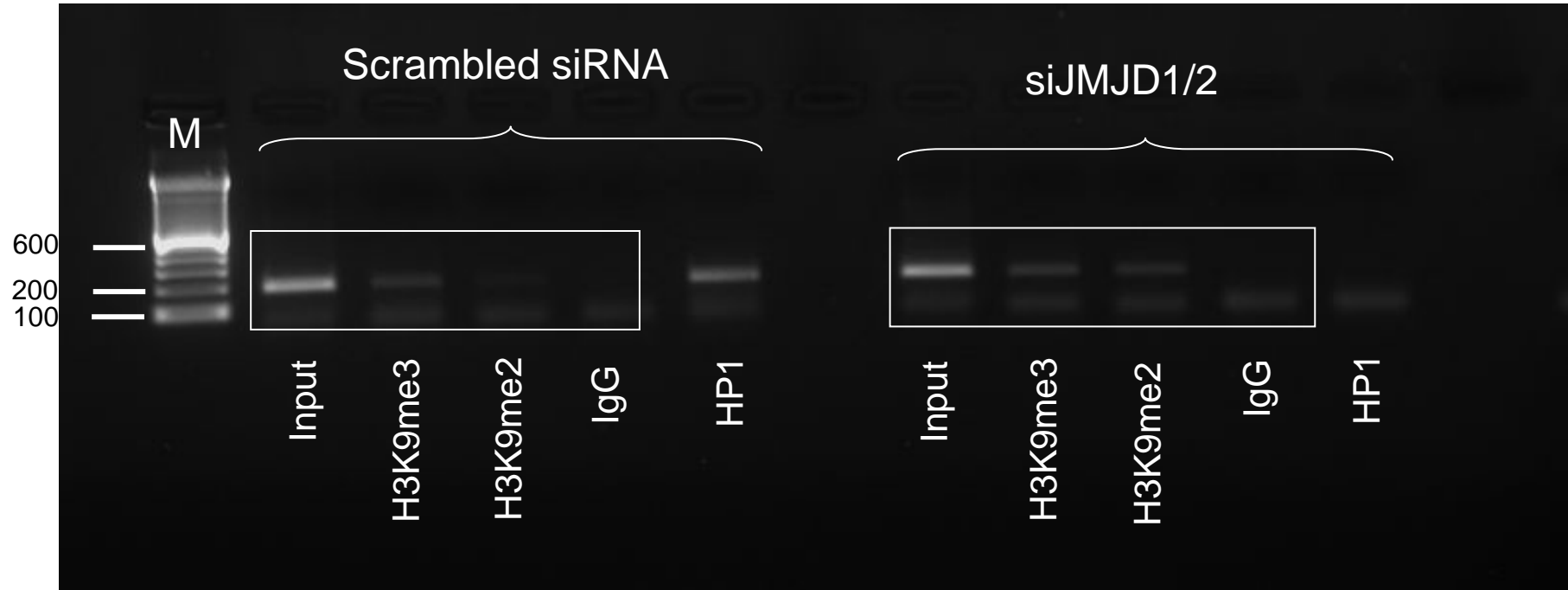
2% Agarose gel  
PCR product for rat ANP-promoter : 192bp

M = 1kb DNA Ladder (Invitrogen)

# Full unedited gel for Figure 6F

Rat BNP promoter Methylation

JMJD1/2 double knock down: siScr und siJMJD

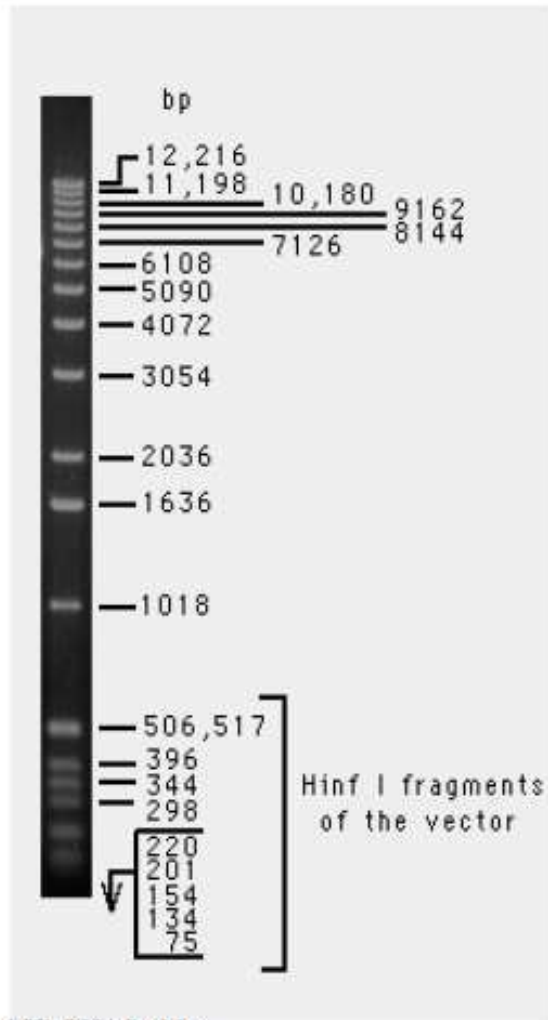


2% Agarose gel  
PCR product for rat BNP-promoter : 182bp

M = 100bp DNA Ladder (Invitrogen)

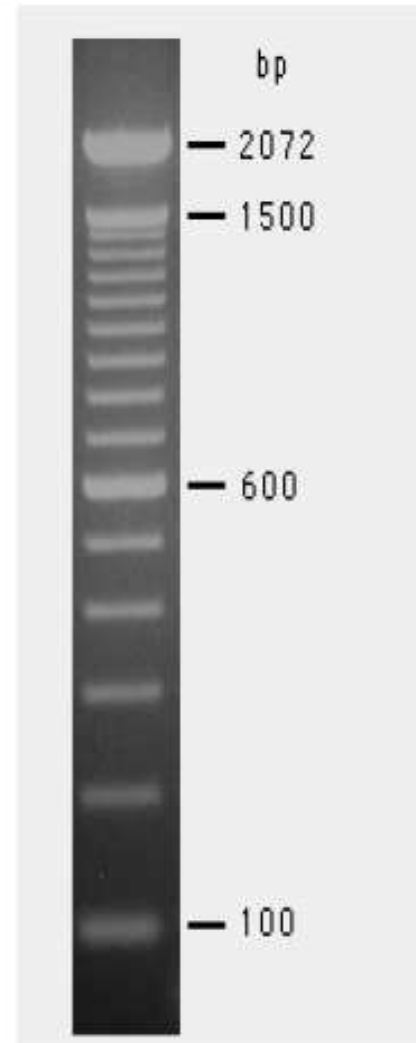


## 1Kb DNA ladder (Invitrogen)



1 Kb DNA Ladder  
0.5 µg/lane  
0.9% agarose gel  
stained with ethidium bromide

## 100bp DNA ladder (Invitrogen)



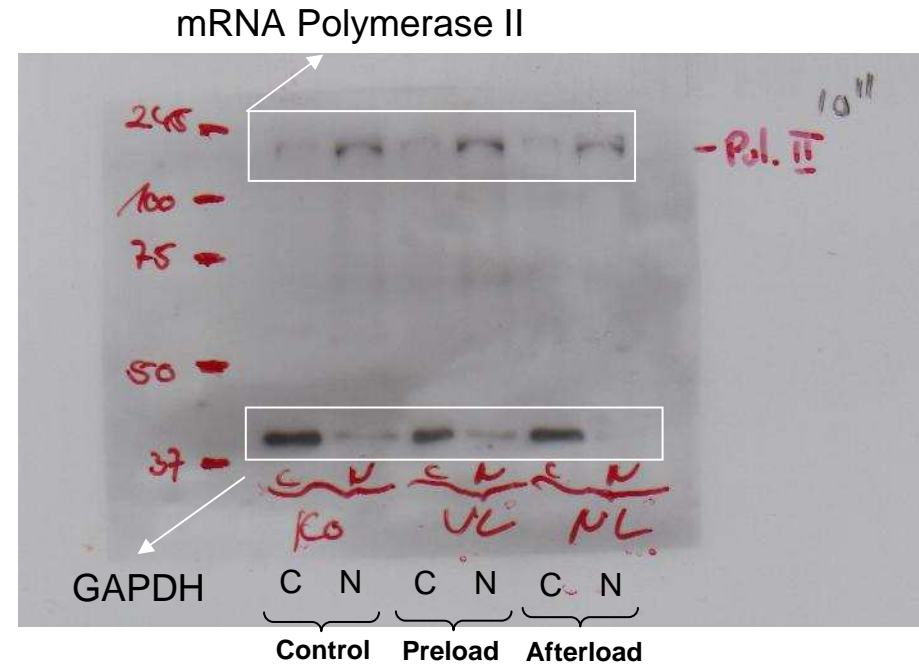
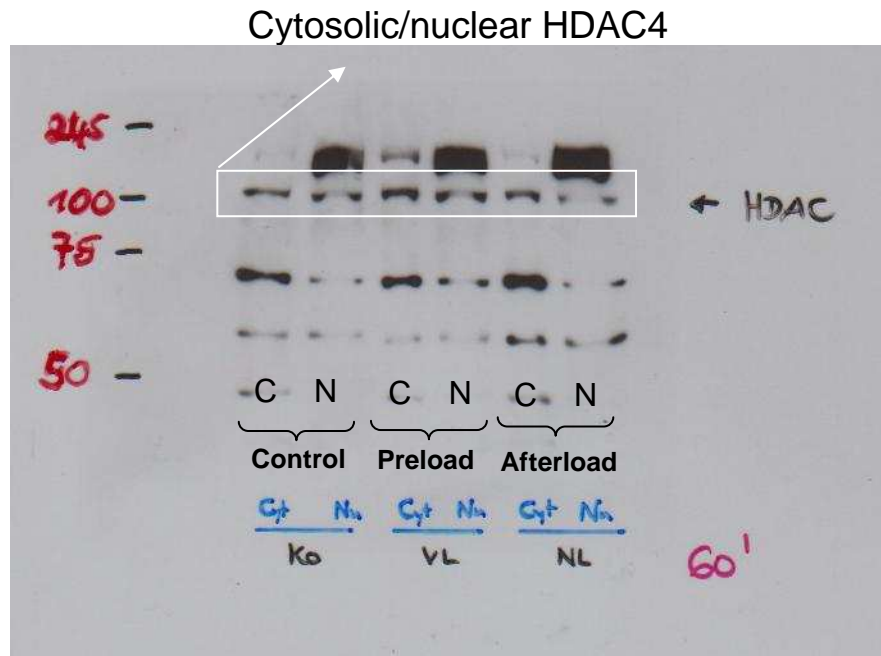
100 bp DNA Ladder  
0.5 µg/lane  
2% agarose gel stained with ethidium bromide.

Note:  
Durin  
100 t  
borat

Part c  
band

Refer:  
1. Hsi  
2. Stel  
3. Jorc

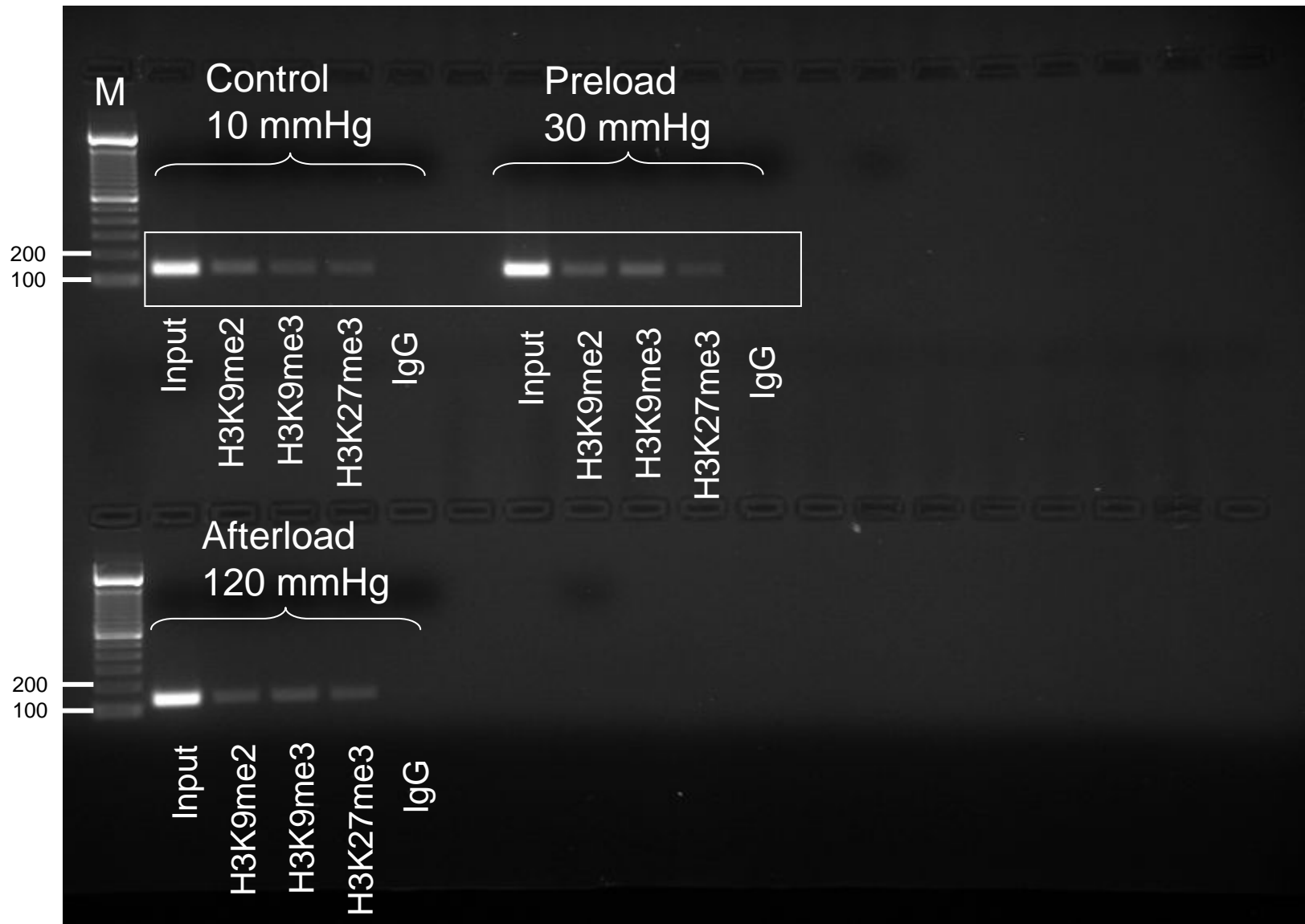
# Full unedited Figure 7



C= cytosolic protein fraction  
N= nuclear protein fraction

# Full unedited gel for Figure 8A

## Mouse GAPDH promoter Methylation at H3K9 and H3K27

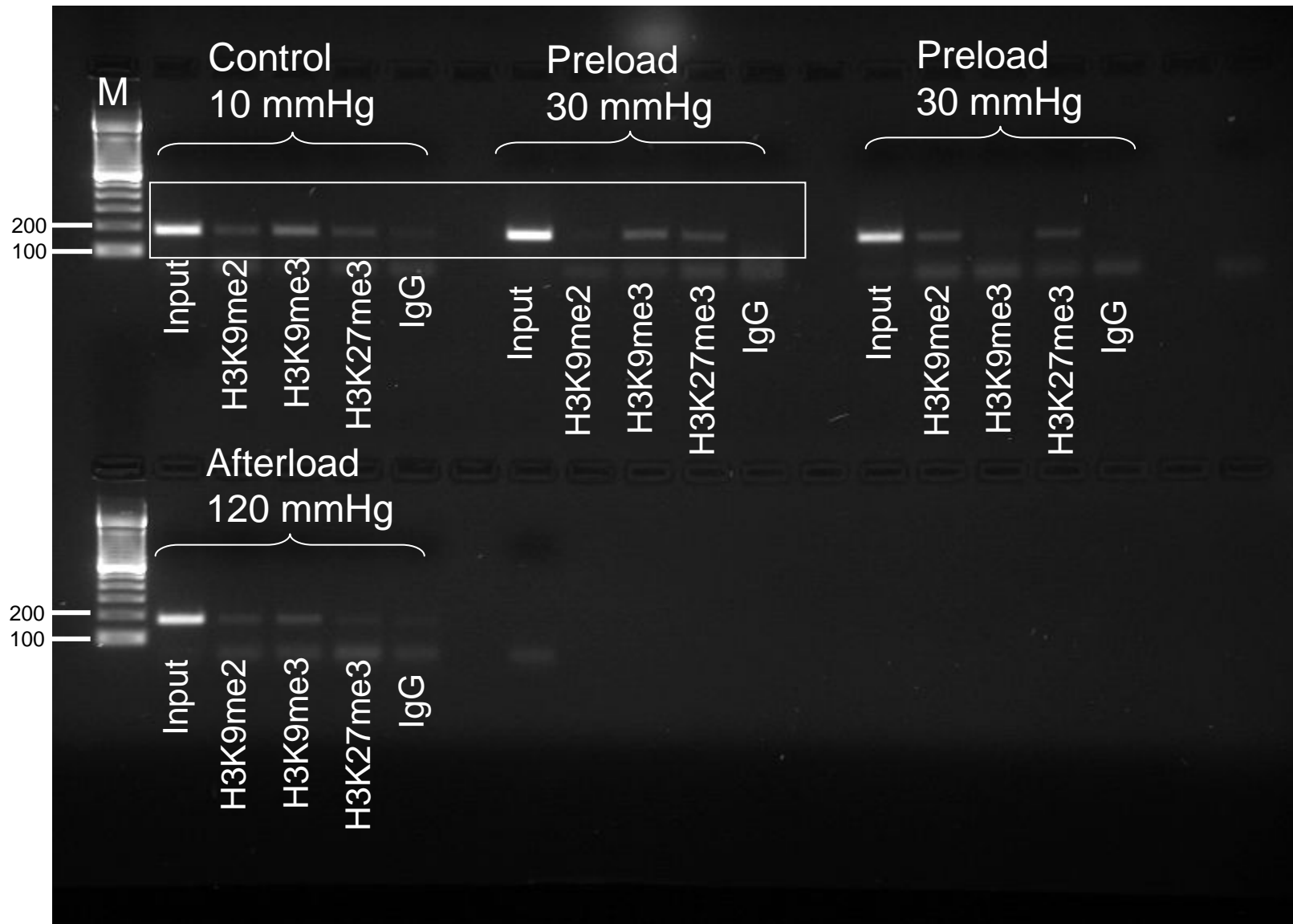


2% Agarose gel, PCR product for mouse GAPDH-promoter : 133bp

M = 100 bp DNA Ladder (Invitrogen)

# Full unedited gel for Figure 8A

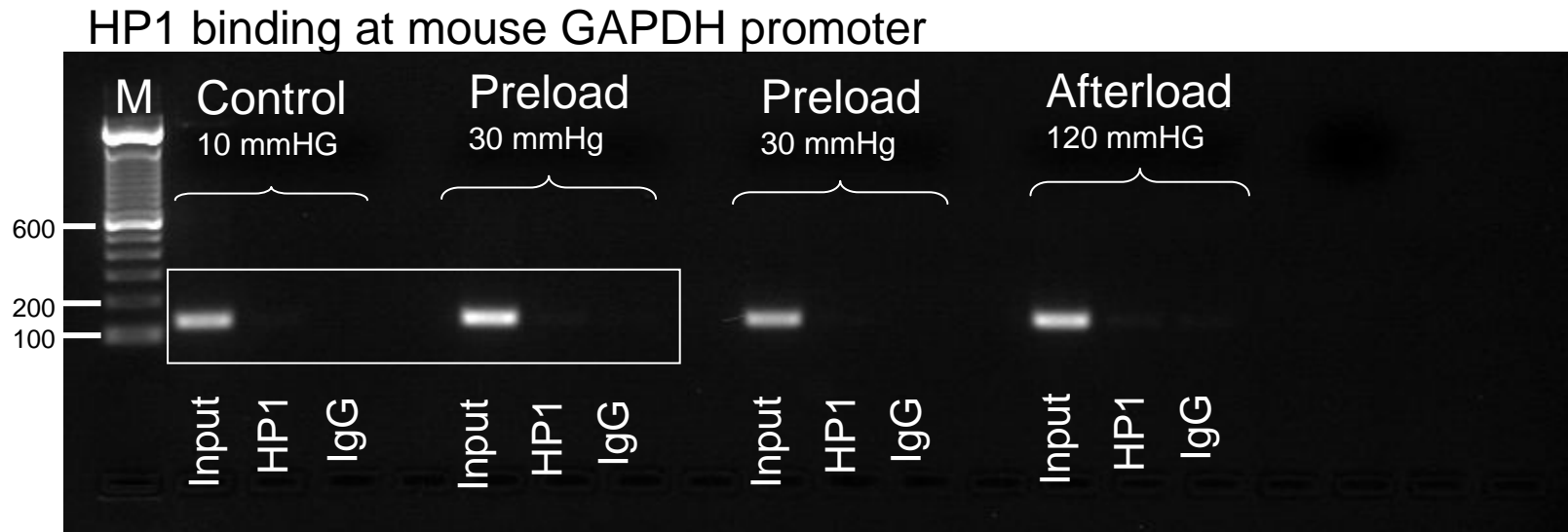
## Mouse ANP promoter Methylation at H3K9 and H3K27



2% Agarose gel, PCR product for mouse ANP-promoter : 181bp

M = 100 bp DNA Ladder (Invitrogen)

# Full unedited gel for Figure 8B

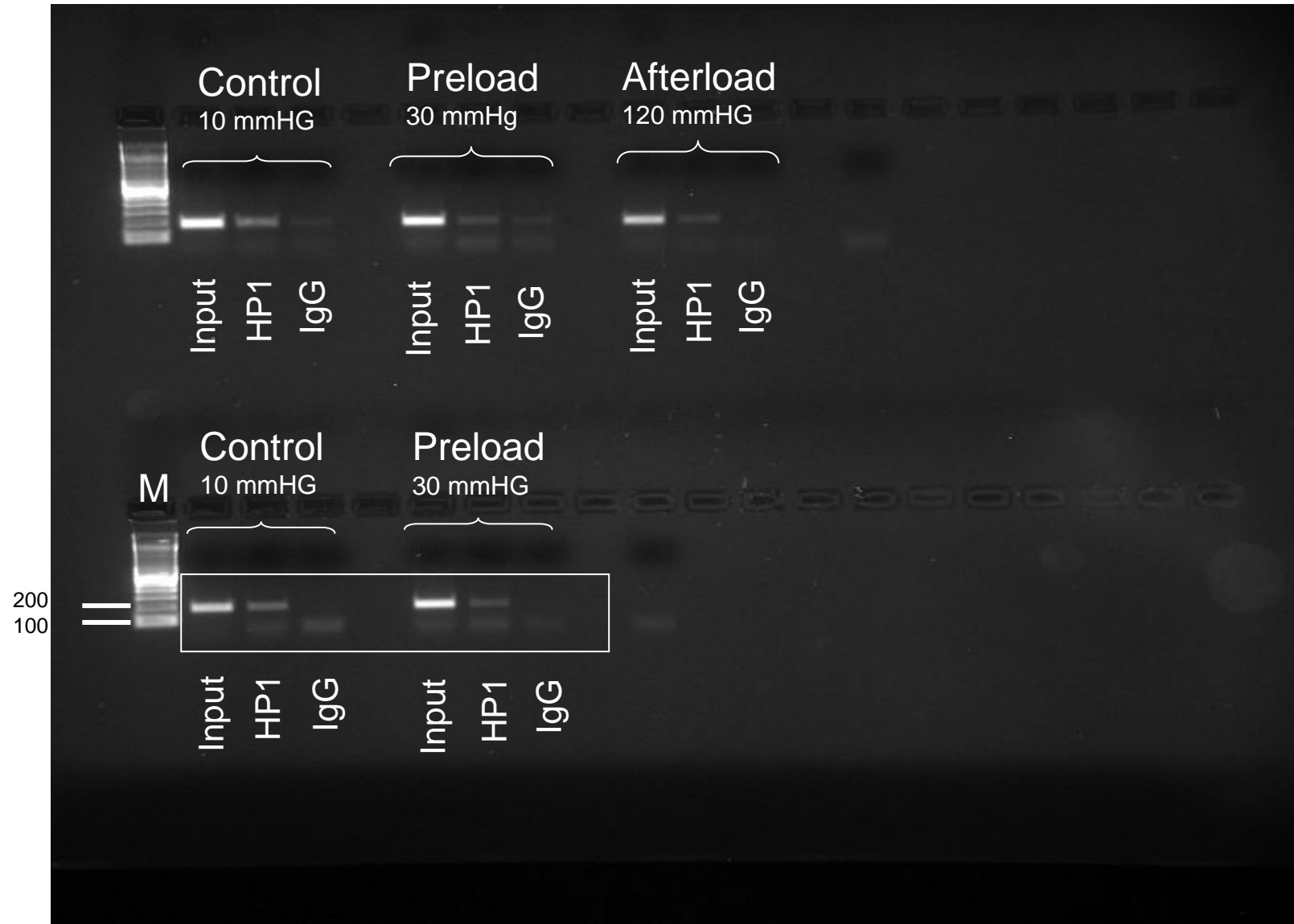


2% Agarose gel, PCR product for mouse GAPDH-promoter : 133bp

M = 100 bp DNA Ladder (Invitrogen)

# Full unedited gel for Figure 8B

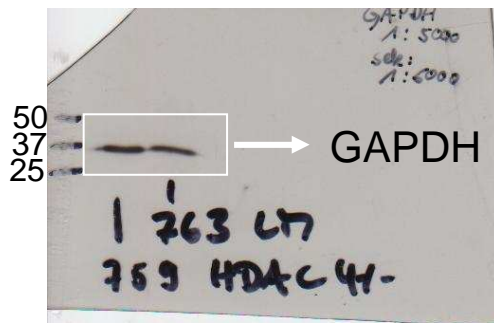
## HP1 binding at mouse ANP promoter



2% Agarose gel, PCR product for mouse ANP-promoter : 181bp

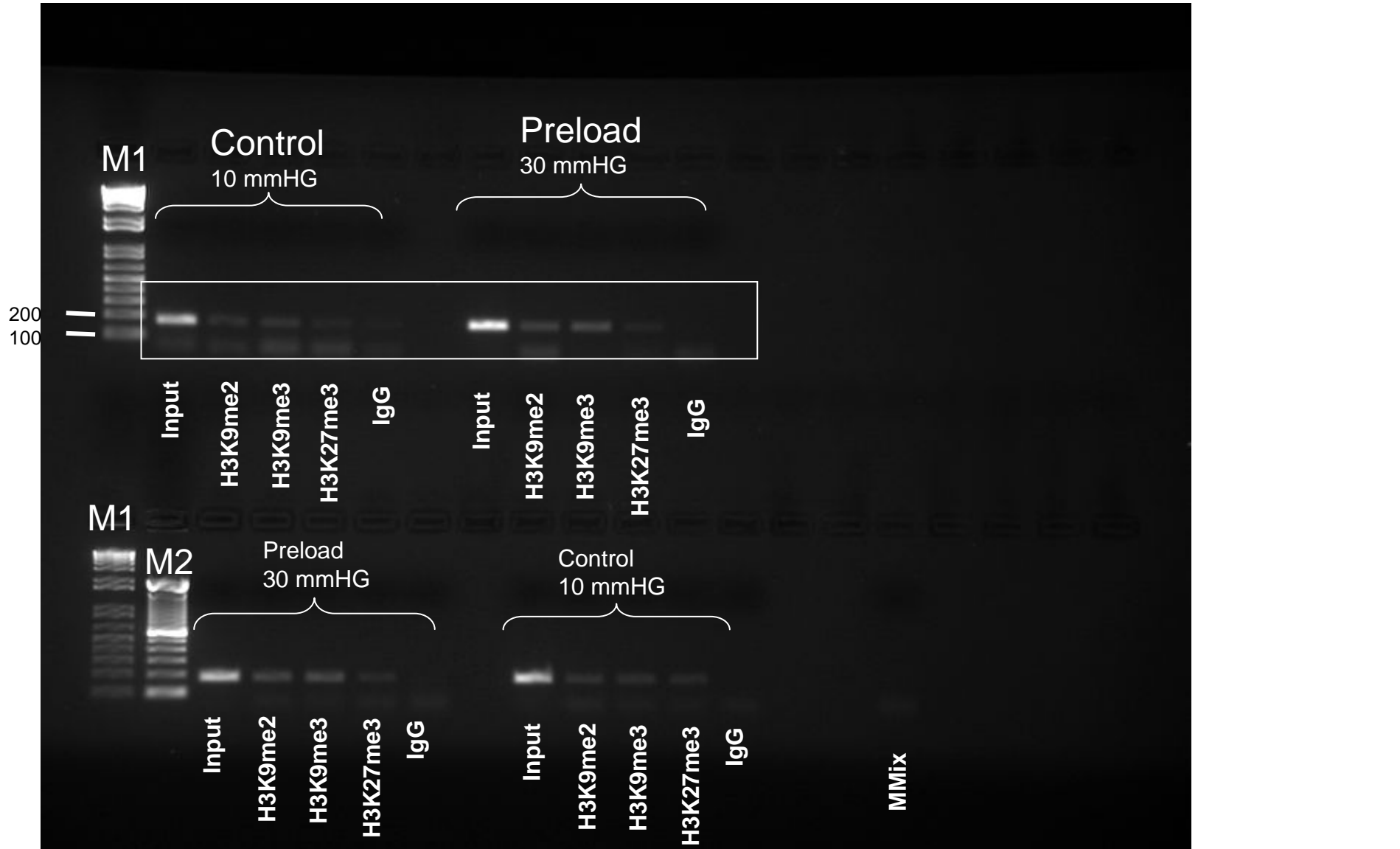
M = 100 bp DNA Ladder (Invitrogen)

# Full unedited gels for Figure 9A



# Full unedited gel for Figure 9E

## Mouse ANP-promoter Methylation at H3K9 and H3K27 in HDAC4-CKO mice



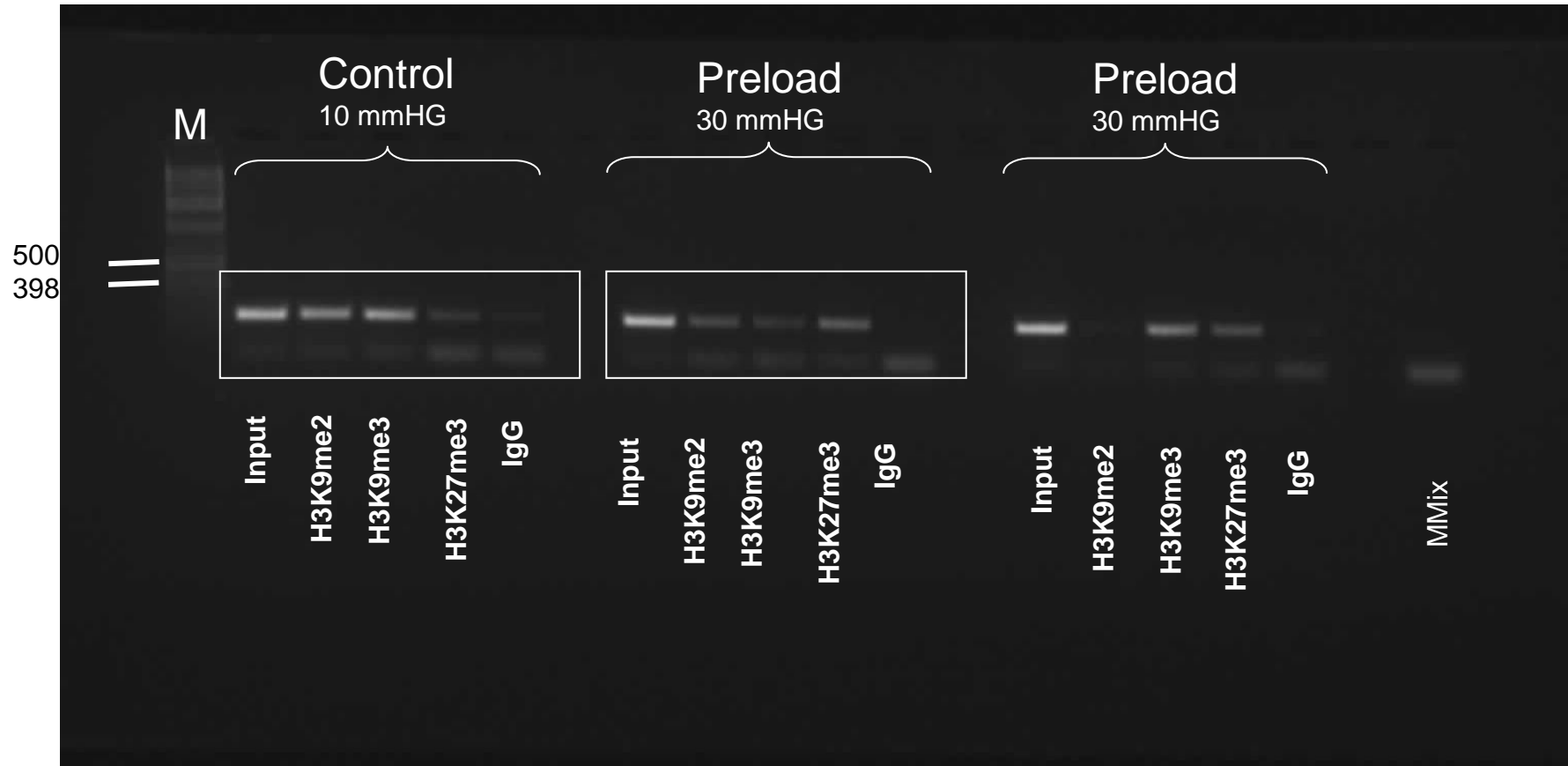
2% Agarose gel, PCR product for mouse ANP-promoter : 181bp

M1 = 1Kb plus DNA Ladder (Invitrogen)  
M2 = 100bp DNA Ladder



# Full unedited gel for Figure 9E

## Mouse ANP promoter Methylation at H3K9 and H3K27 in HDAC4-Littermates

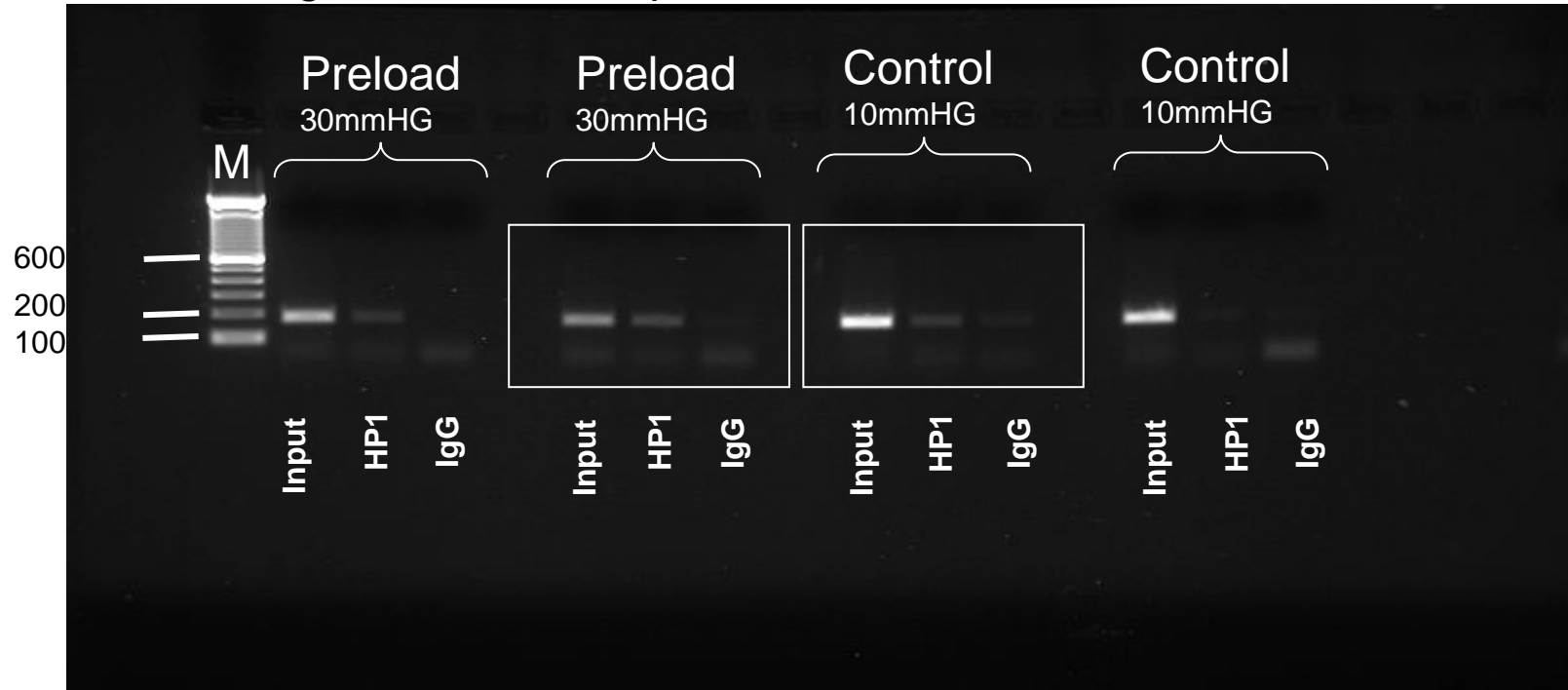


2% Agarose gel, PCR product for mouse ANP-promoter : 181bp

M = 1kb DNA Ladder (Invitrogen)

# Full unedited gel for Figure 9I

## HP1 binding at mouse ANP promoter in HDAC4-CKO

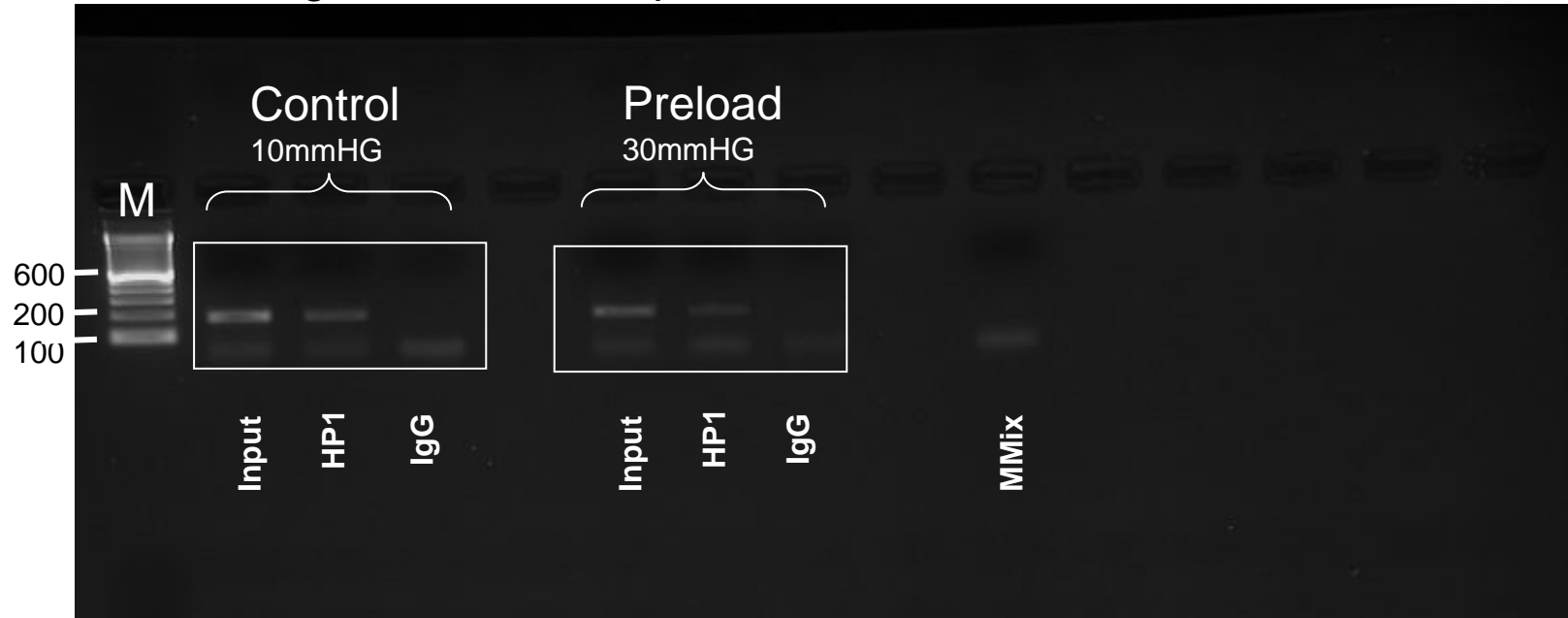


2% Agarose gel, PCR product for mouse ANP-promoter : 181bp

M = 100 bp DNA Ladder (Invitrogen)

# Full unedited gel for Figure 9I

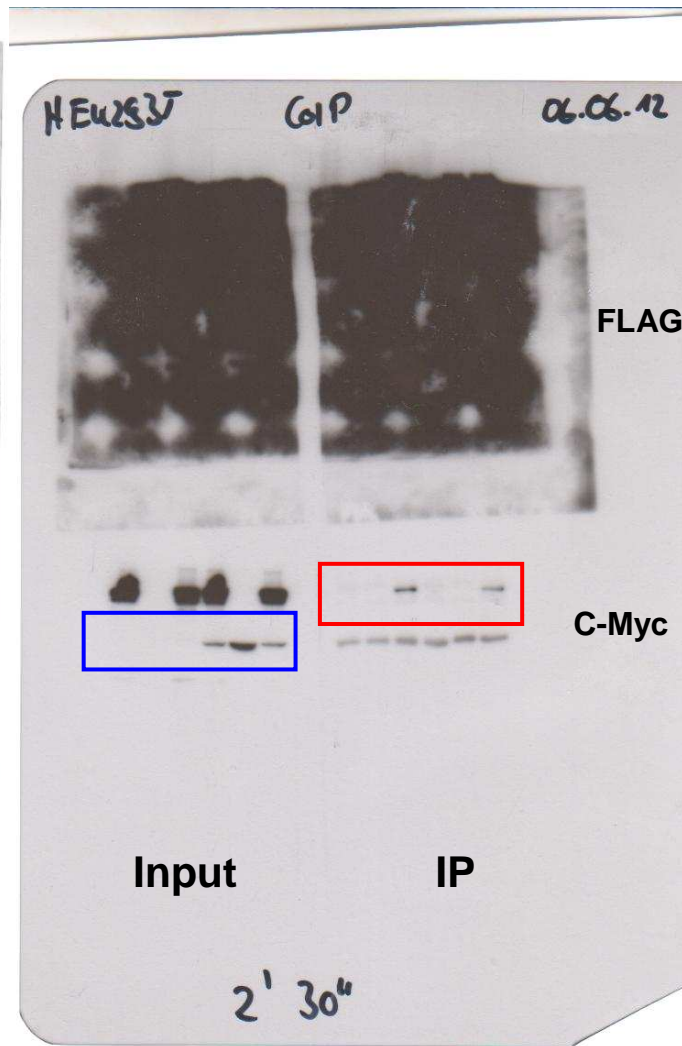
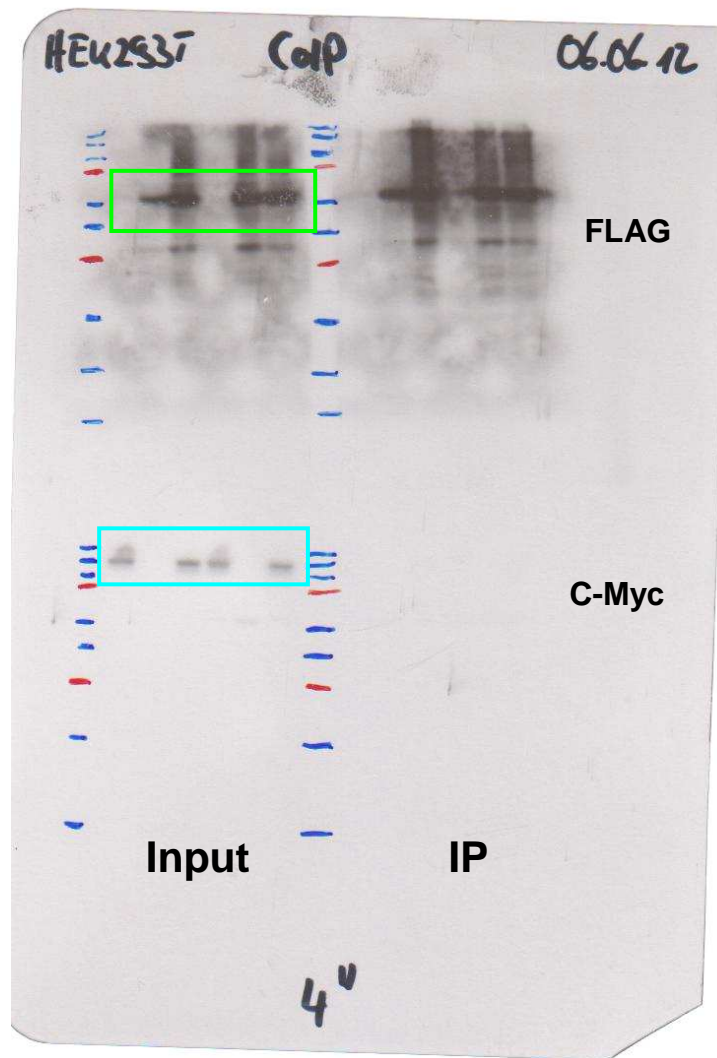
## HP1 binding at mouse ANP promoter in HDAC4-Littermate



2% Agarose gel, PCR product for mouse ANP-promoter : 181bp

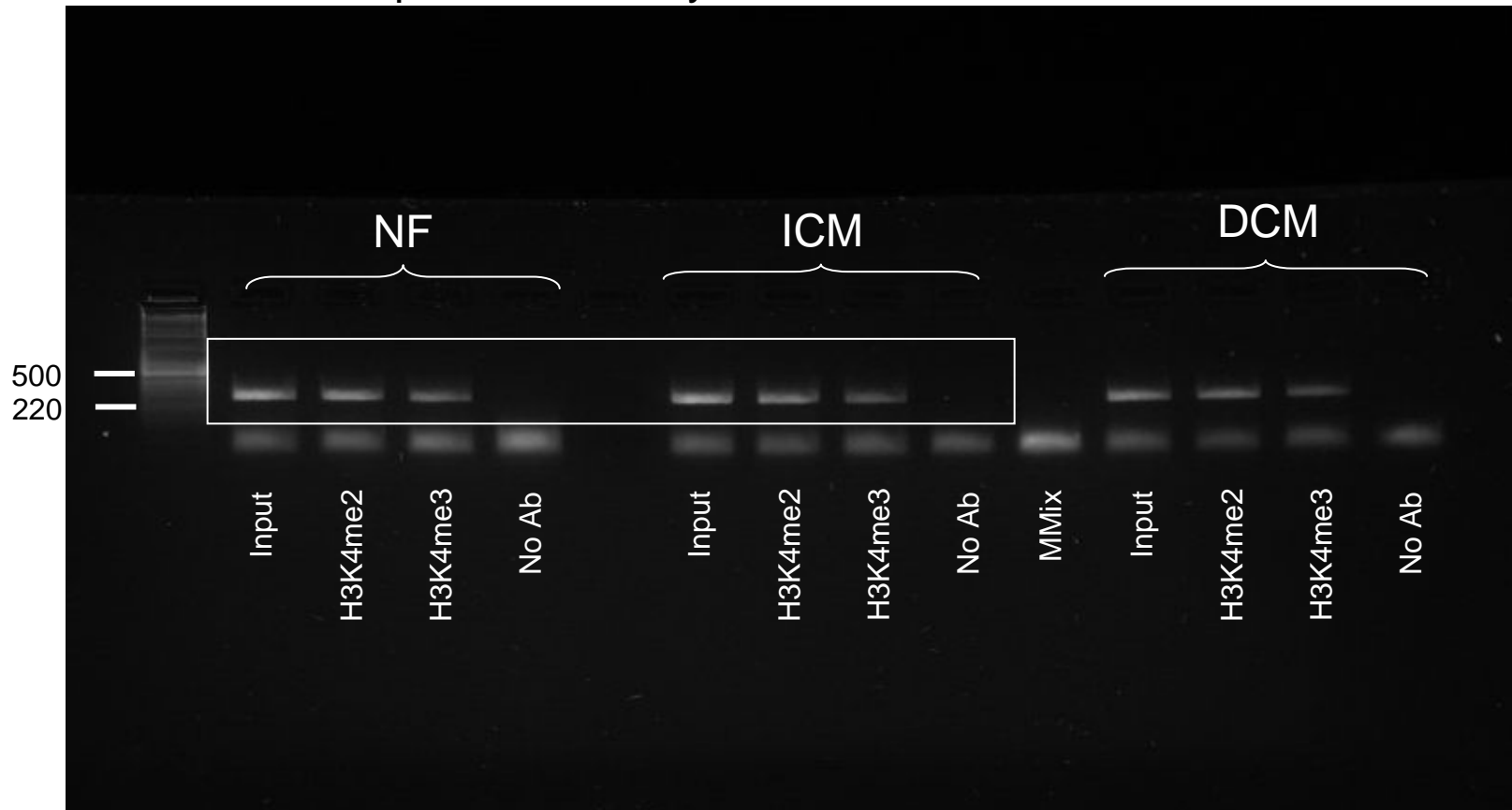
M = 100 bp DNA Ladder (Invitrogen)

Full unedited gel for Figure 10D



# Full unedited gel for Figure S2B

## Human GAPDH promoter Methylation at H3K4



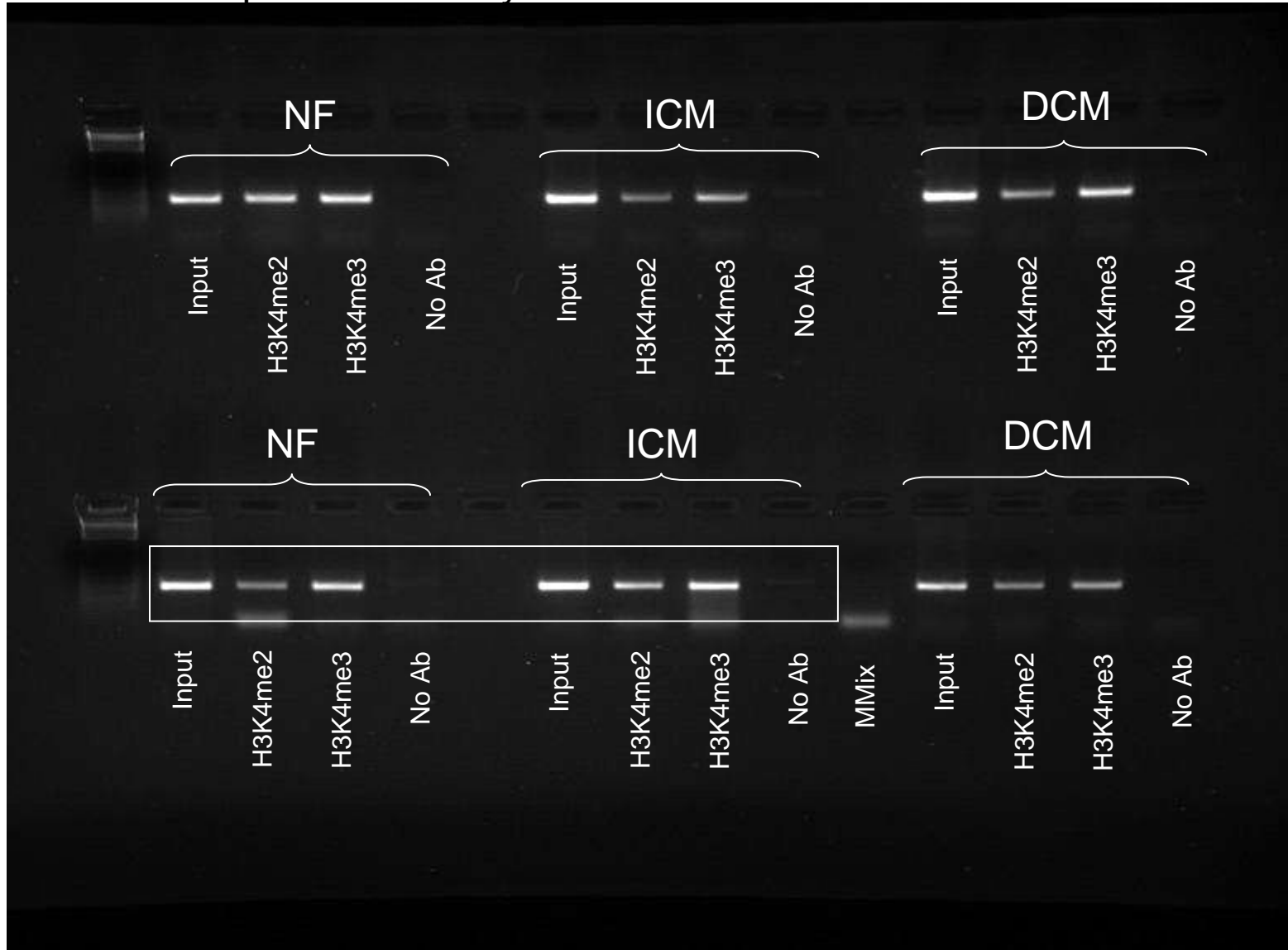
M = 1Kb DNA Ladder (Invitrogen)

2% Agarose gel

PCR product for GAPDH-promoter : 262bp

Full unedited gel for Figure S2B

Human ANP promoter methylation at H3K4

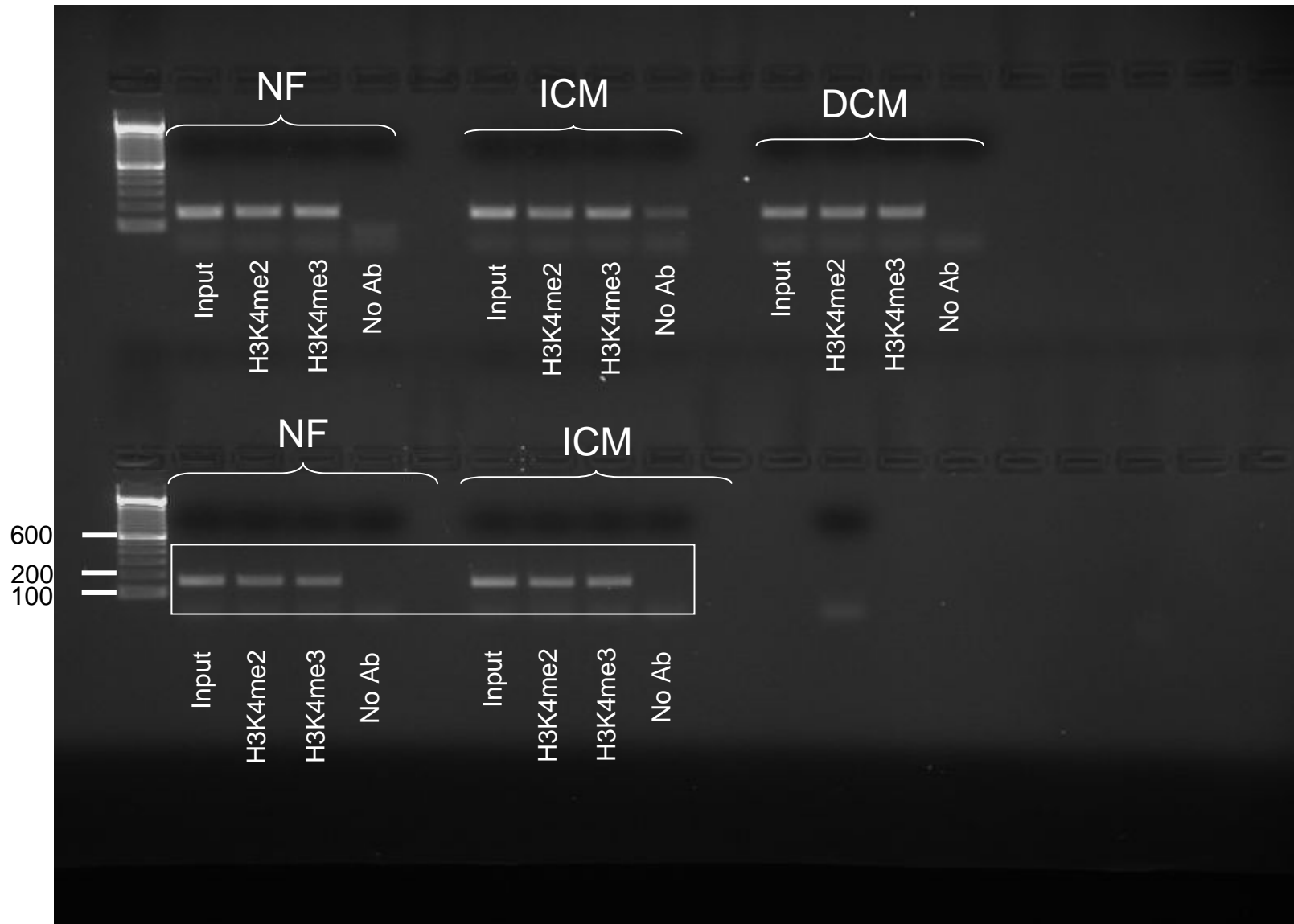


2% Agarose gel, PCR product for ANP-promoter : 299bp

M = 1Kb DNA Ladder (Invitrogen)

# Full unedited gel for Figure S2B

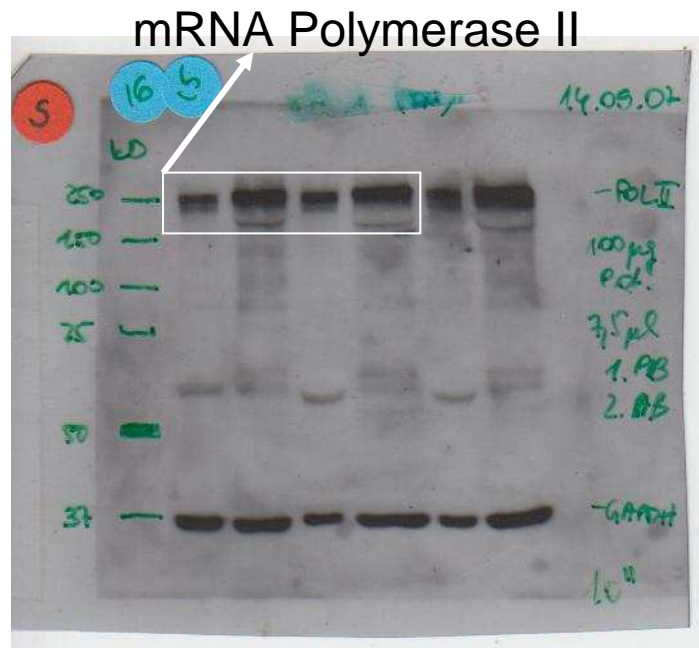
## Human BNP promoter methylation at H3K4



2% Agarose gel, PCR product for BNP-promoter : 150bp

M = 100bp DNA Ladder (Invitrogen)

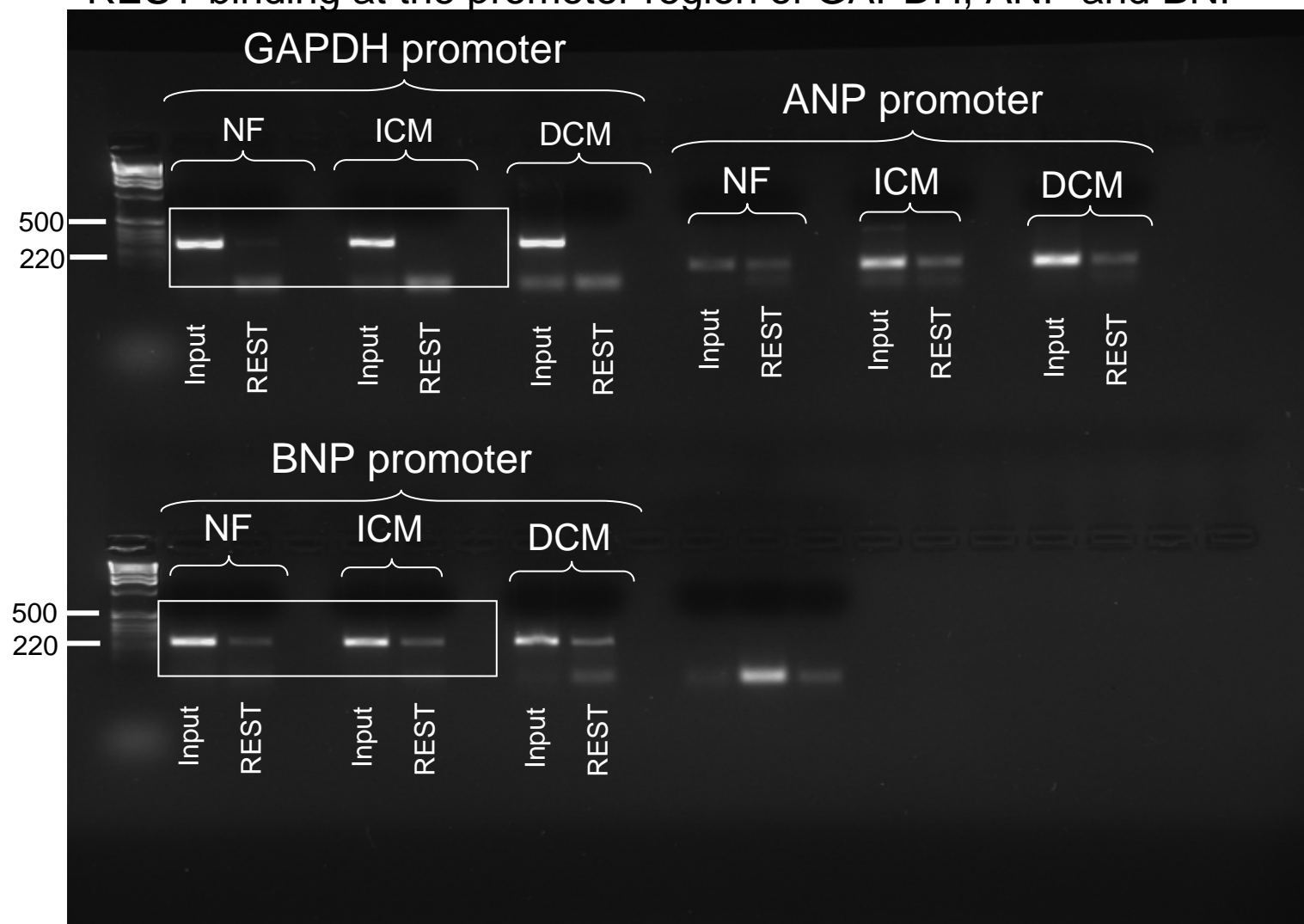
# Full unedited gel for Figure S4B





# Full unedited gel for Figure S4C

## REST binding at the promoter region of GAPDH, ANP and BNP



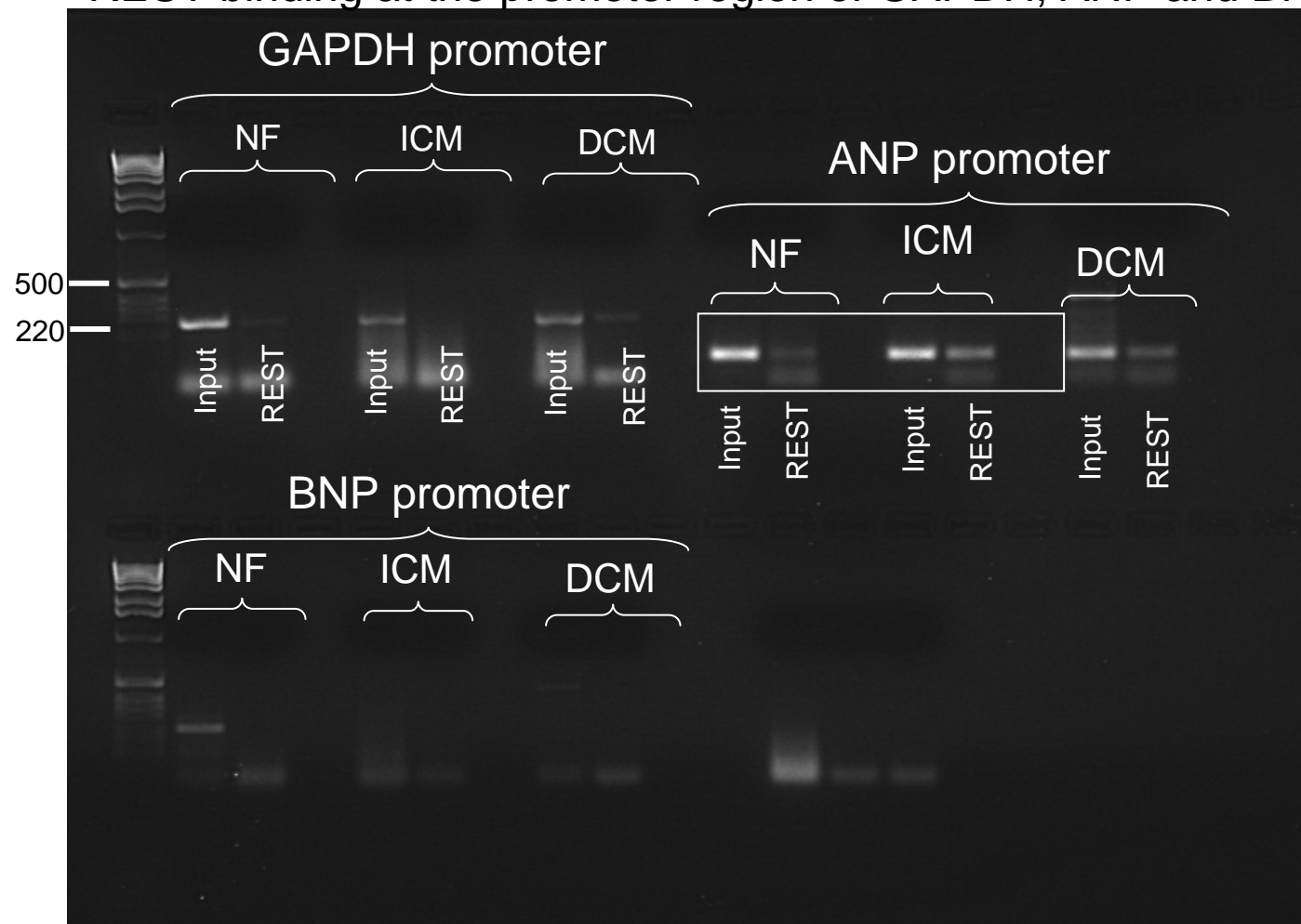
M = 1Kb DNA Ladder (Invitrogen)

2% Agarose gel

PCR product for promoters : 262bp (GAPDH-prom), 112 bp (ANP-prom), 227bp (BNP-prom)

# Full unedited gel for Figure S4C

## REST binding at the promoter region of GAPDH, ANP and BNP



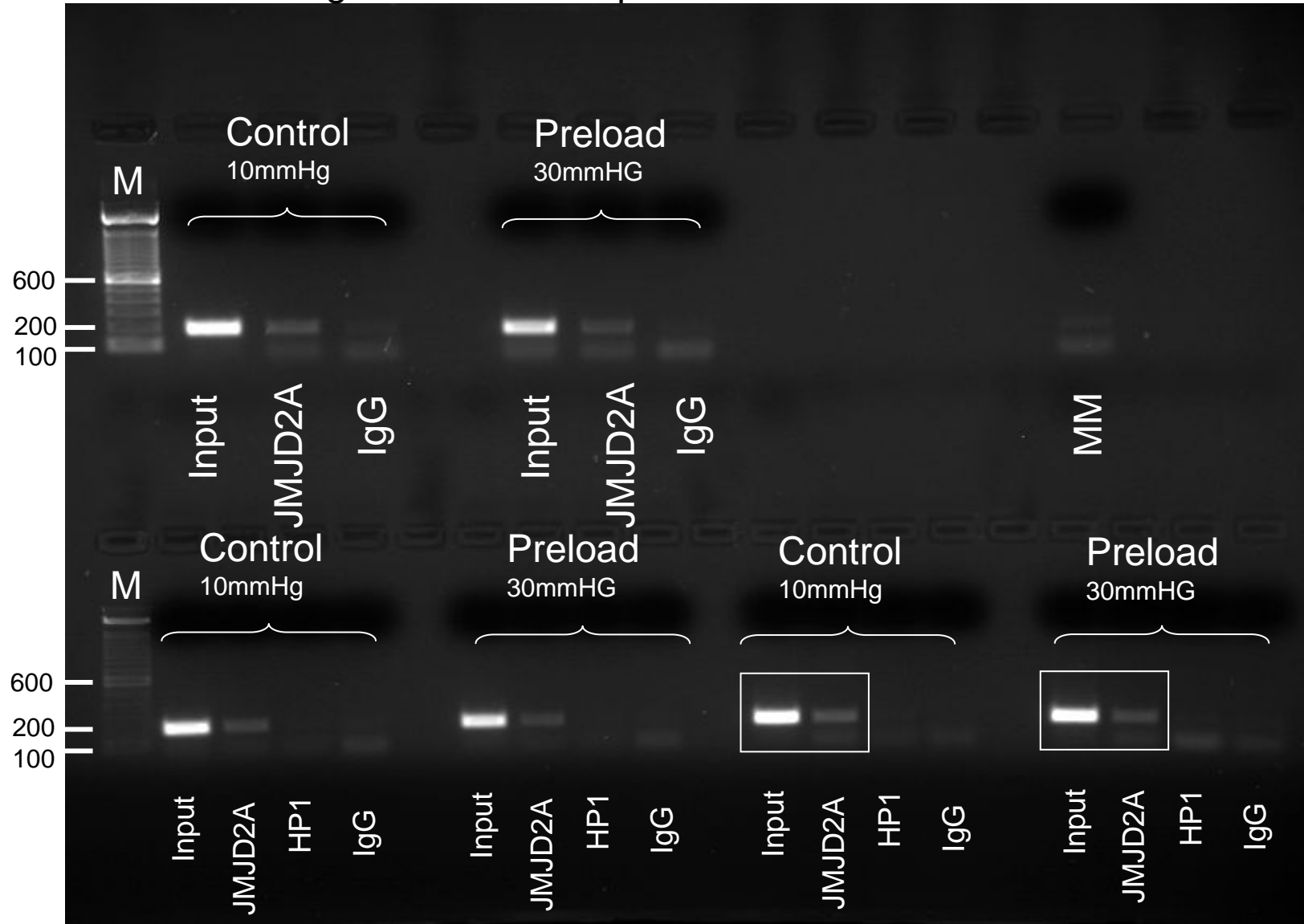
M = 1Kb DNA Ladder (Invitrogen)

2% Agarose gel

PCR product for promoters : 262bp (GAPDH-prom), 112 bp (ANP-prom), 227bp (BNP-prom)

# Full unedited gel for Figure S6

## JMJD2A binding at mouse ANP promoter

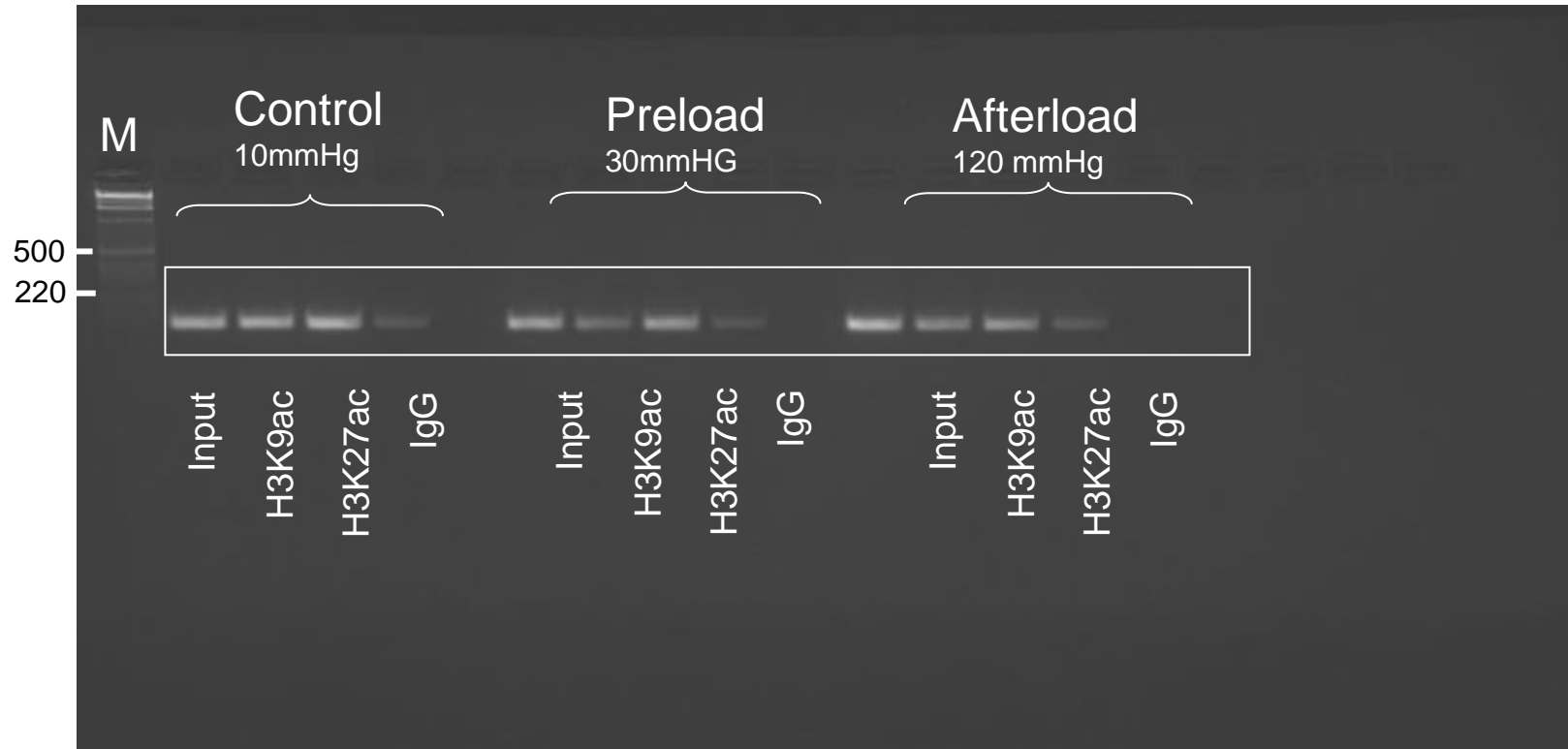


2% Agarose gel  
PCR product for mouse ANP-promoter : 181bp

M = 100bp DNA Ladder (Invitrogen)

# Full unedited Gel for Figure S7A

## Acetylation of mouse GAPDH promoter at H3K9 and H3K27

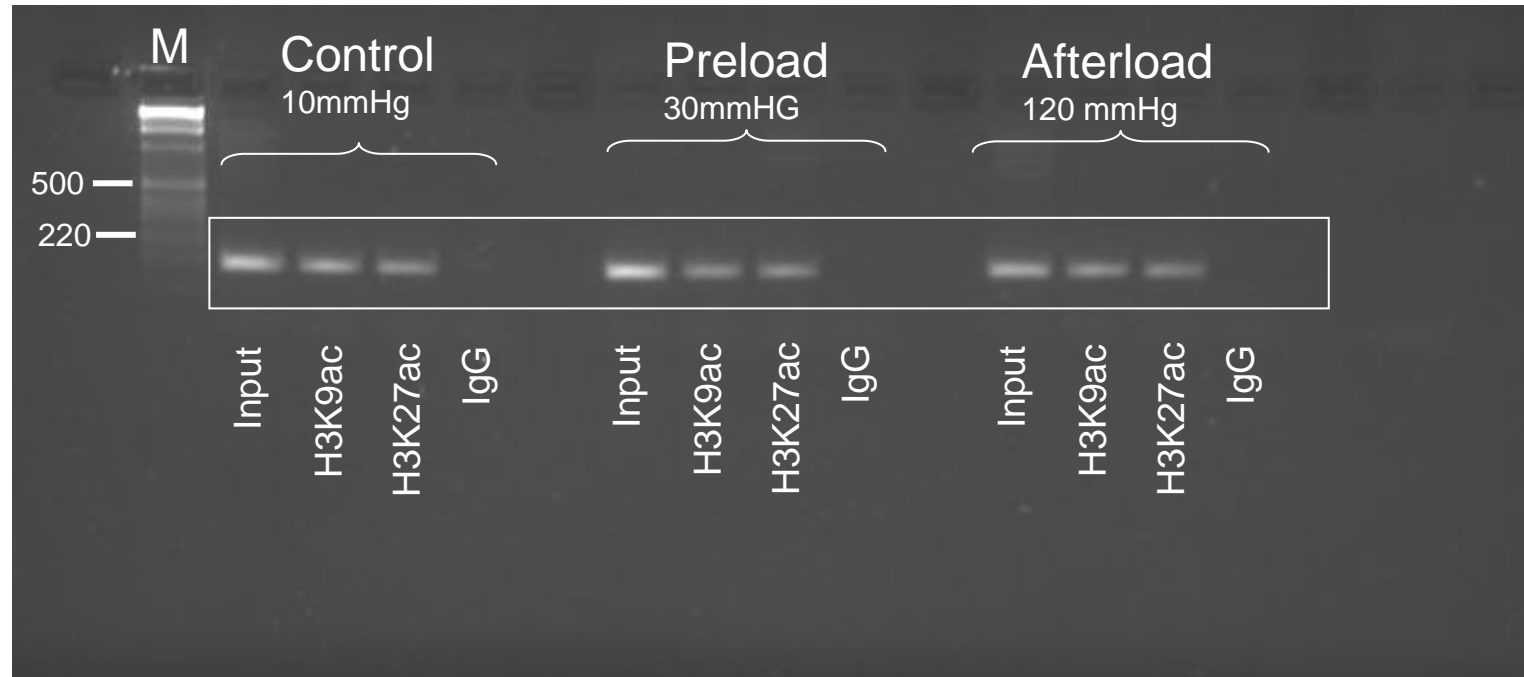


2% Agarose gel  
PCR product for mouse ANP-promoter : 133 bp

M = 1kb DNA Ladder (Invitrogen)

# Full unedited Gel for Figure S7A

## Acetylation of mouse ANP promoter at H3K9 and H3K27

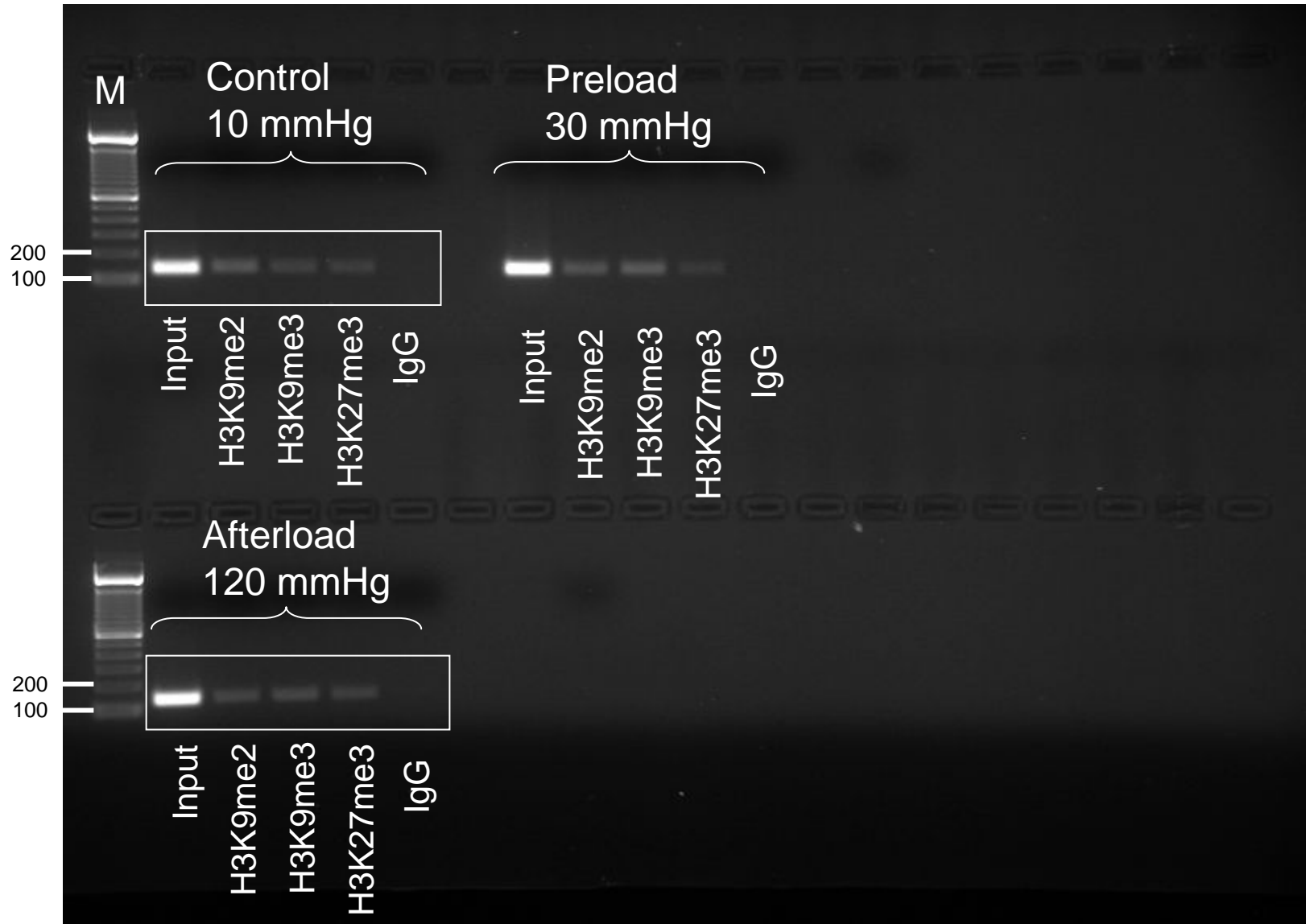


2% Agarose gel  
PCR product for mouse ANP-promoter : 181bp

M = 1kb DNA Ladder (Invitrogen)

# Full unedited gels for Figure S8A

## Mouse GAPDH promoter Methylation at H3K9 and H3K27

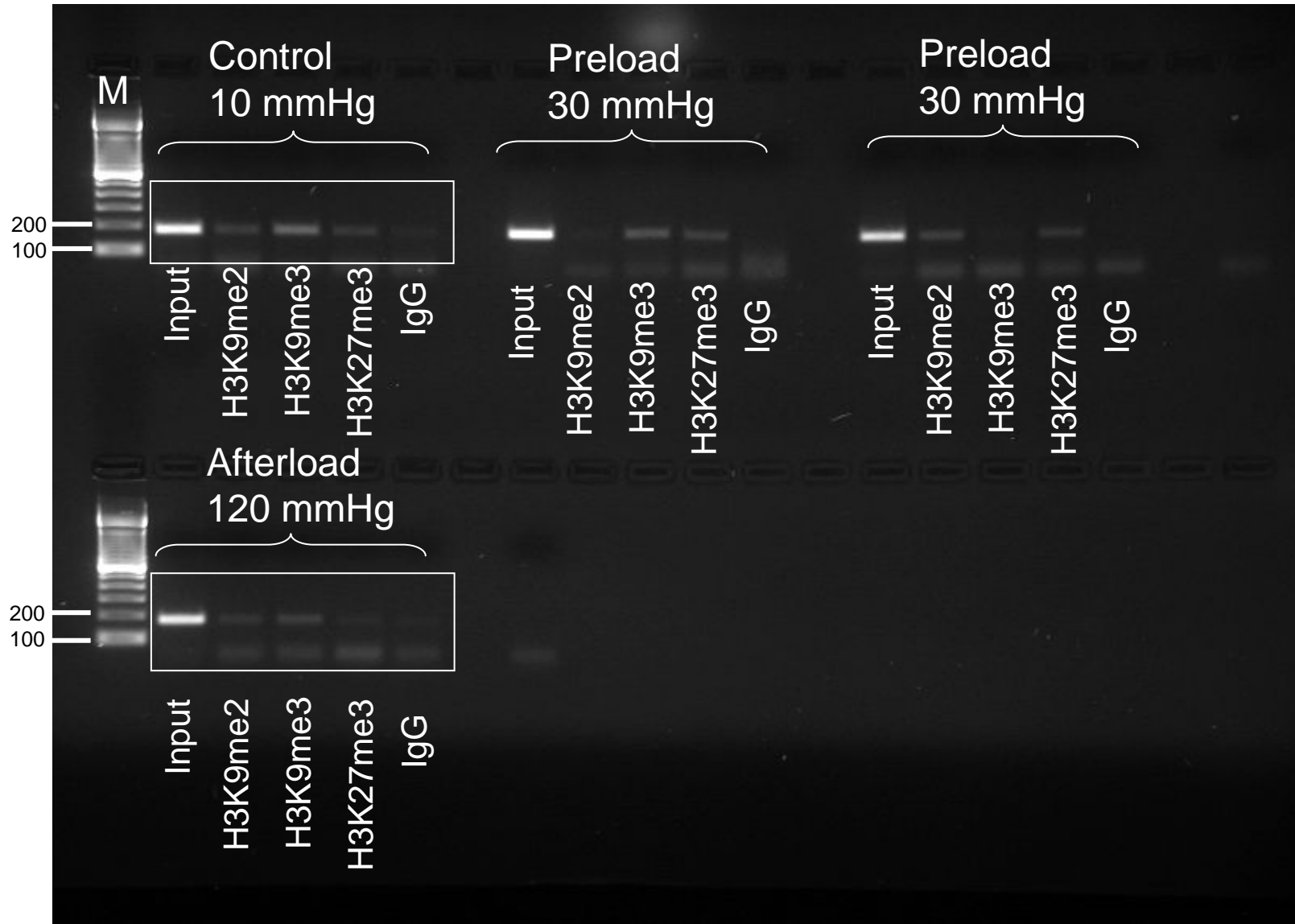


2% Agarose gel, PCR product for mouse GAPDH-promoter : 133bp

M = 100 bp DNA Ladder (Invitrogen)

# Full unedited gels for Figure S8A

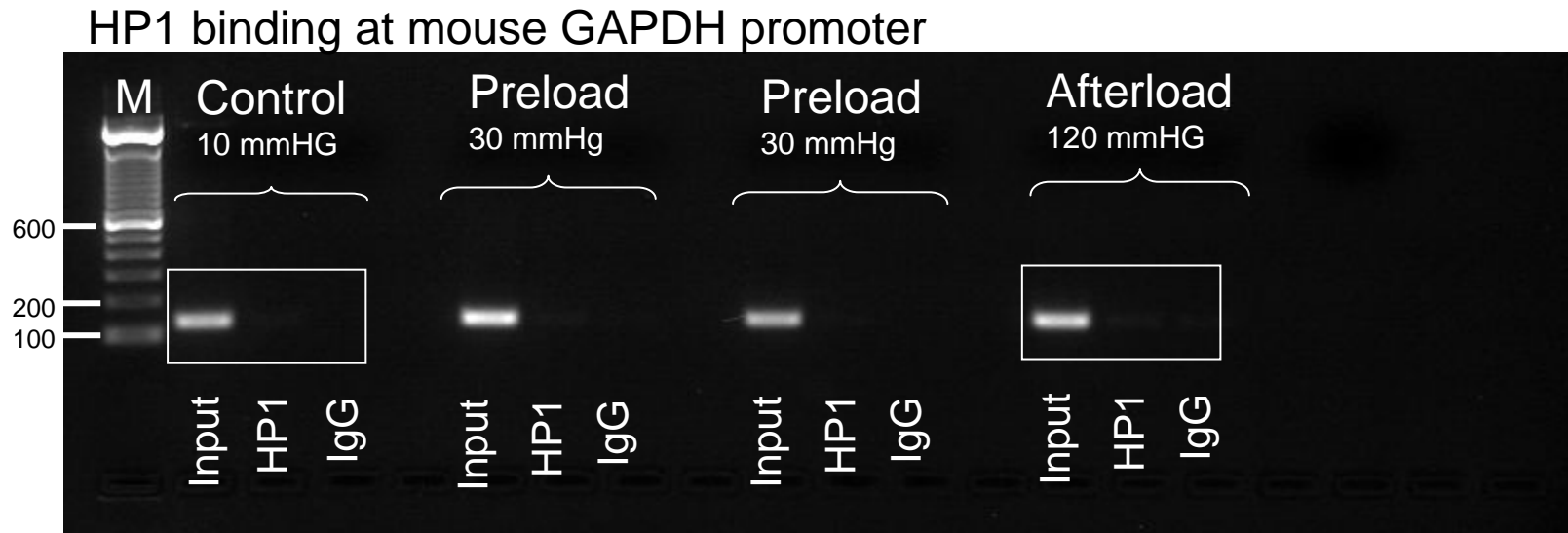
## Mouse ANP promoter Methylation at H3K9 and H3K27



2% Agarose gel, PCR product for mouse ANP-promoter : 181bp

M = 100 bp DNA Ladder (Invitrogen)

# Full unedited gels for Figure S8B



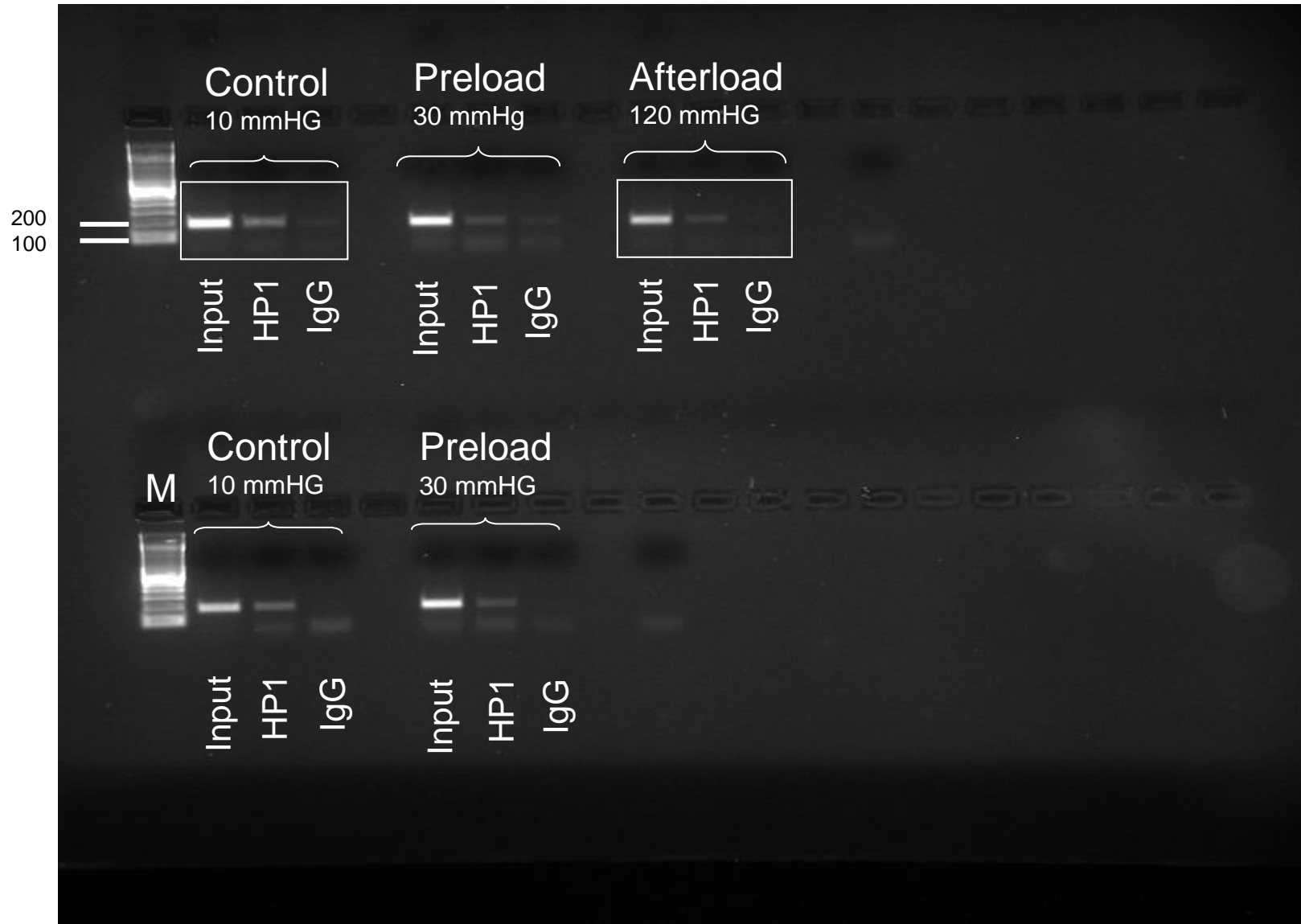
2% Agarose gel, PCR product for mouse GAPDH-promoter : 133bp

M = 100 bp DNA Ladder (Invitrogen)



# Full unedited gels for Figure S8B

## HP1 binding at mouse ANP promoter

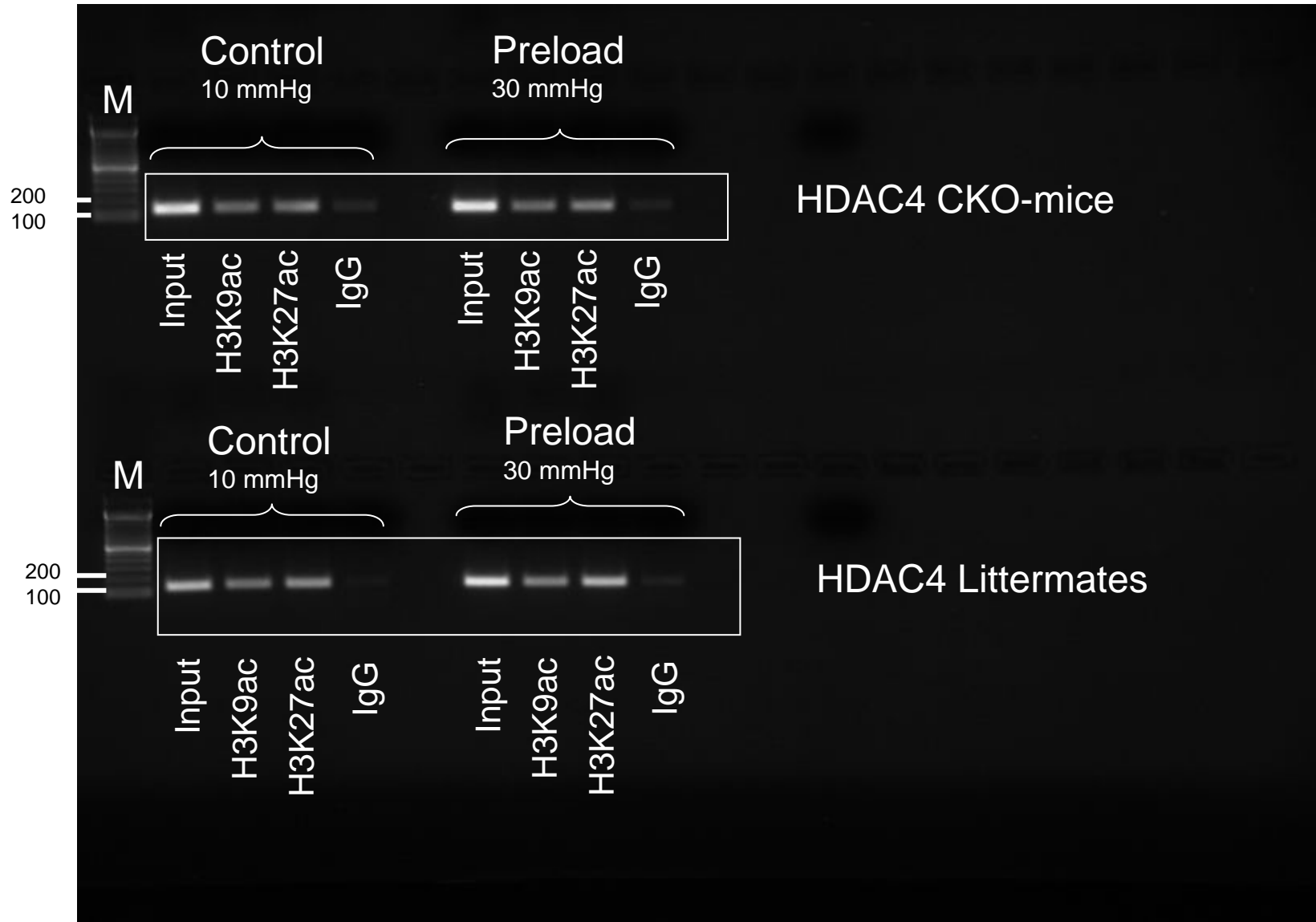


2% Agarose gel, PCR product for mouse ANP-promoter : 181bp

M = 100 bp DNA Ladder (Invitrogen)

# Full unedited gels for Figure S9A

## Mouse GAPDH promoter acetylation at H3K9 and H3K27

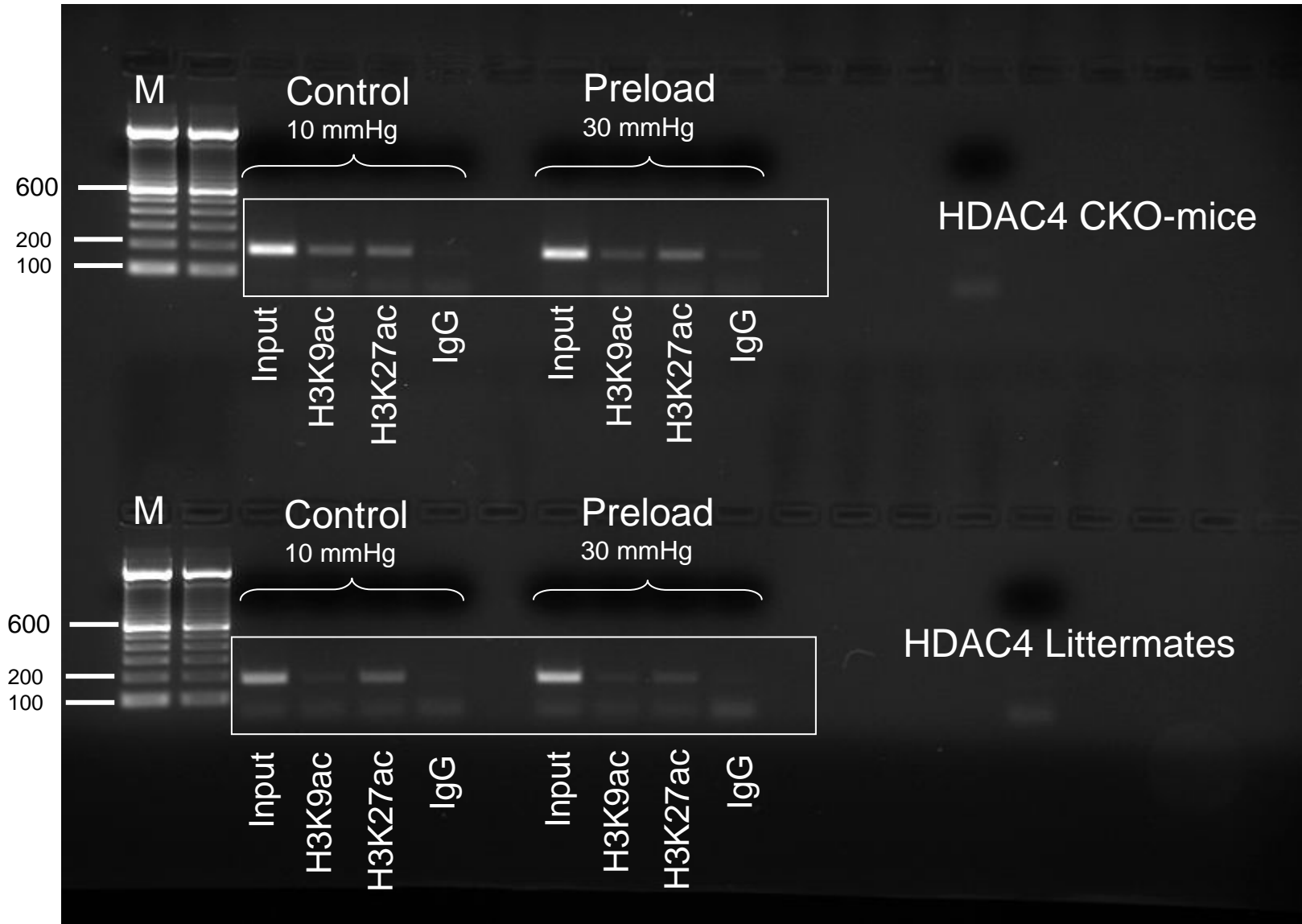


2% Agarose gel, PCR product for mouse GAPDH-promoter : 133bp

M = 100 bp DNA Ladder (Invitrogen)

Full unedited gels for Figure S9A

Mouse ANP promoter acetylation at H3K9 and H3K27



2% Agarose gel, PCR product for mouse ANP-promoter : 181bp

M = 100 bp DNA Ladder (Invitrogen)